Biological motors

18.S995 - L10

Reynolds numbers

$$Re = \frac{\rho U L}{\mu} = \frac{UL}{\nu}$$

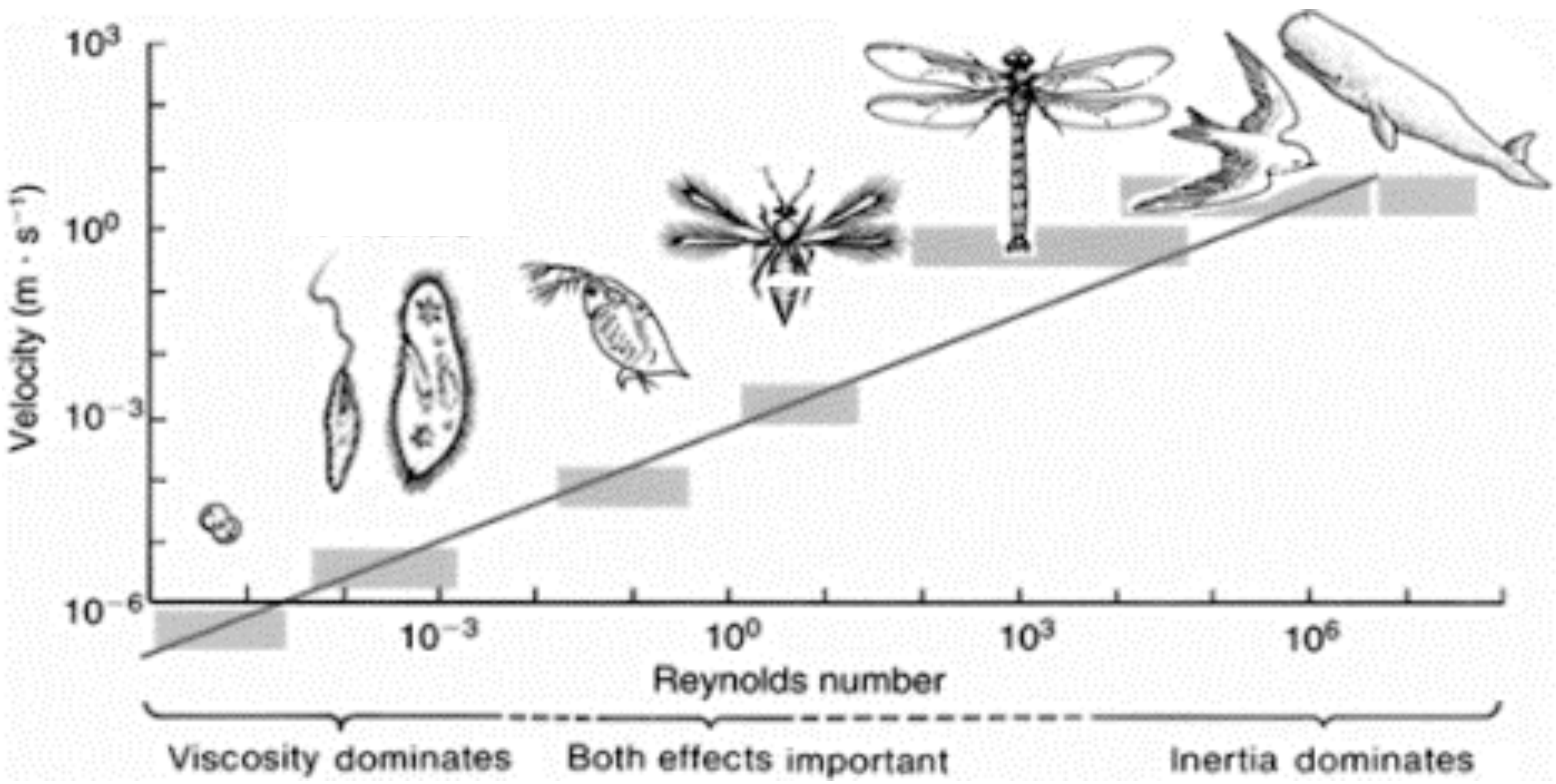

E.coli (non-tumbling HCB 437)

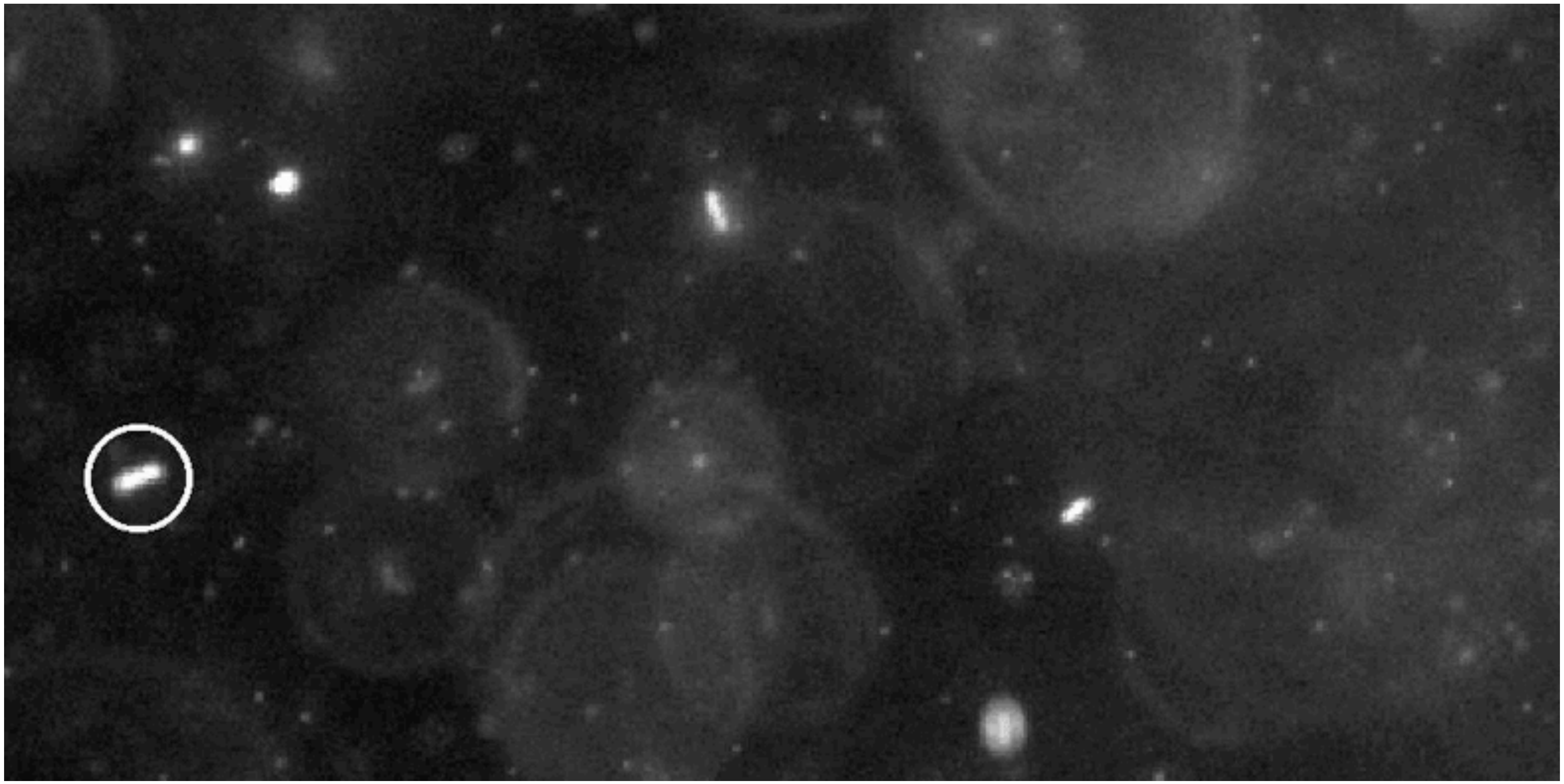

Drescher, Dunkel, Ganguly, Cisneros, Goldstein (2011) PNAS

dunkel@math.mit.edu

Bacterial motors

movie: V. Kantsler

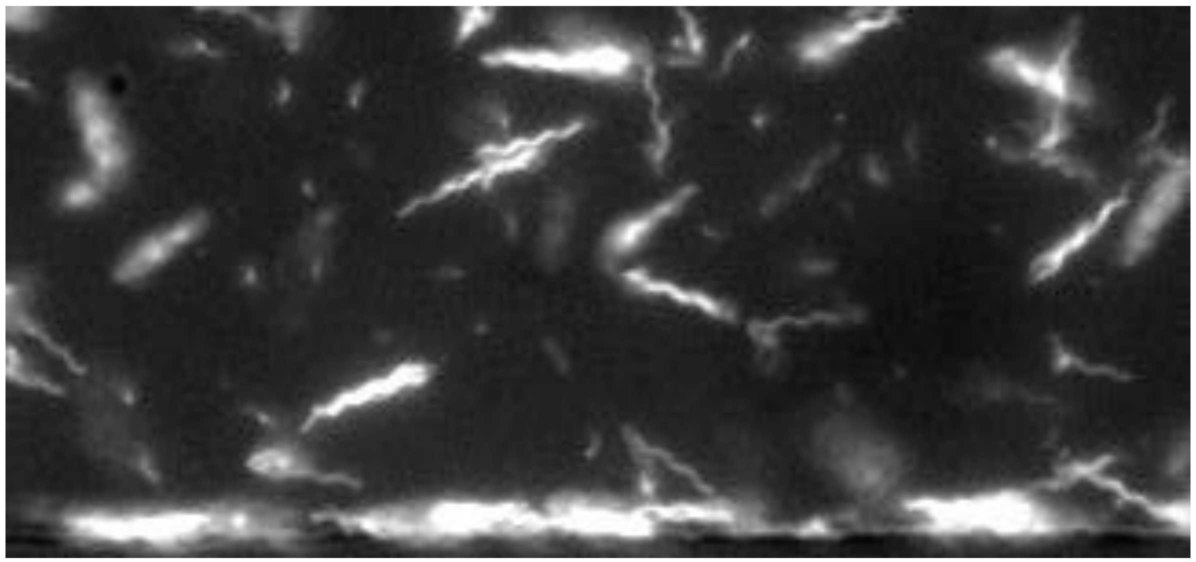

~20 parts

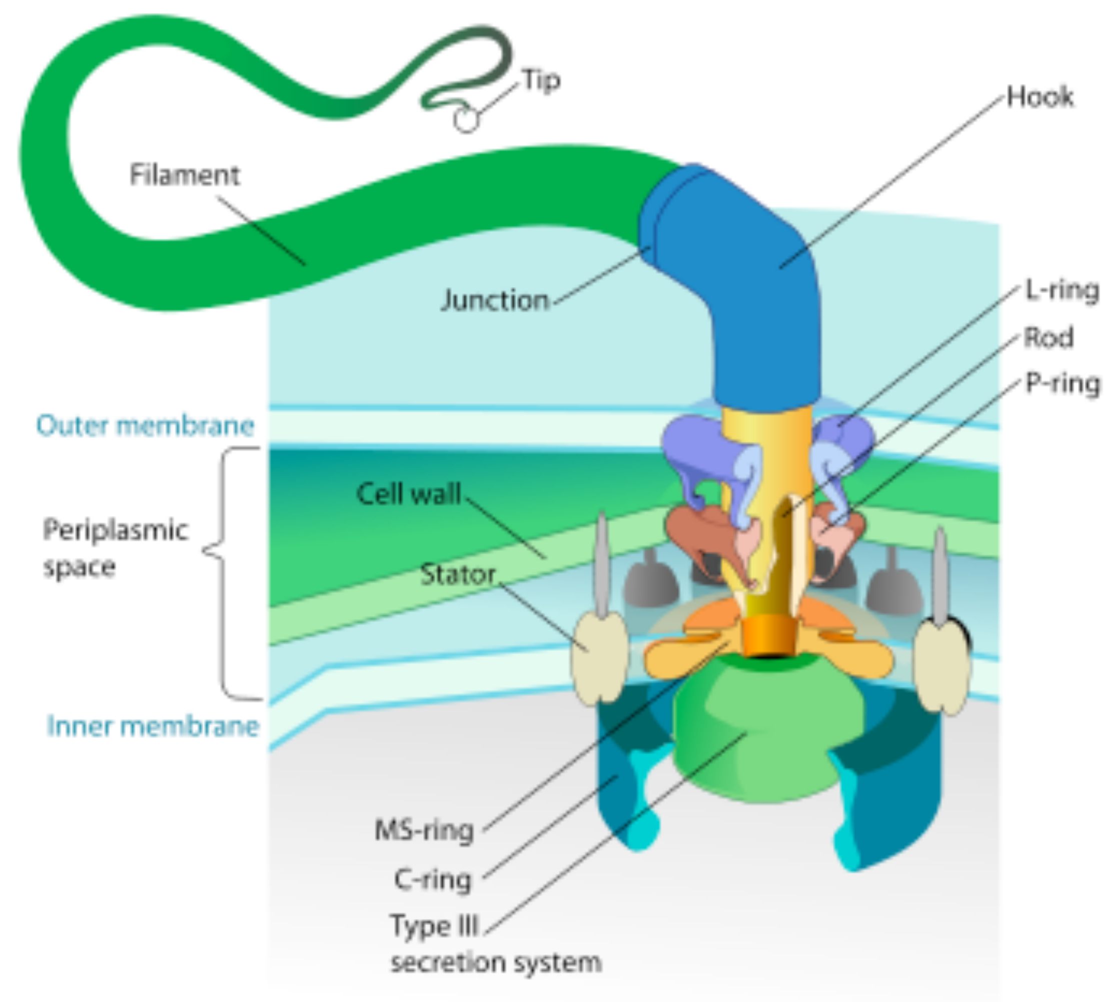

source: wiki

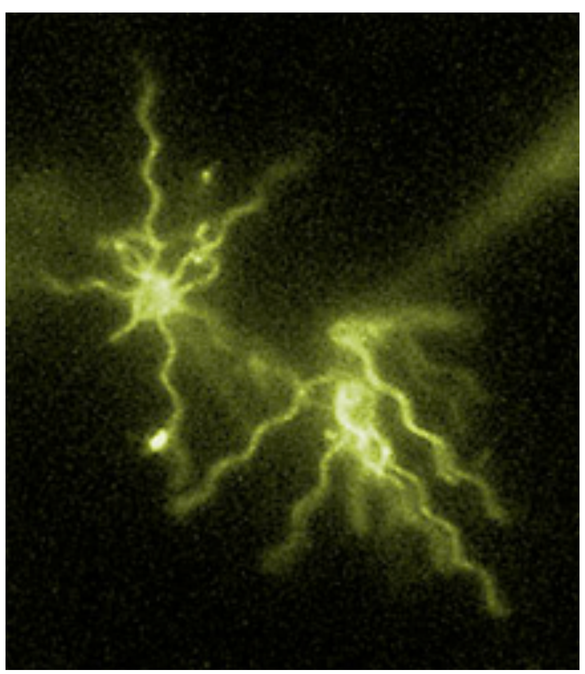

Berg (1999) Physics Today

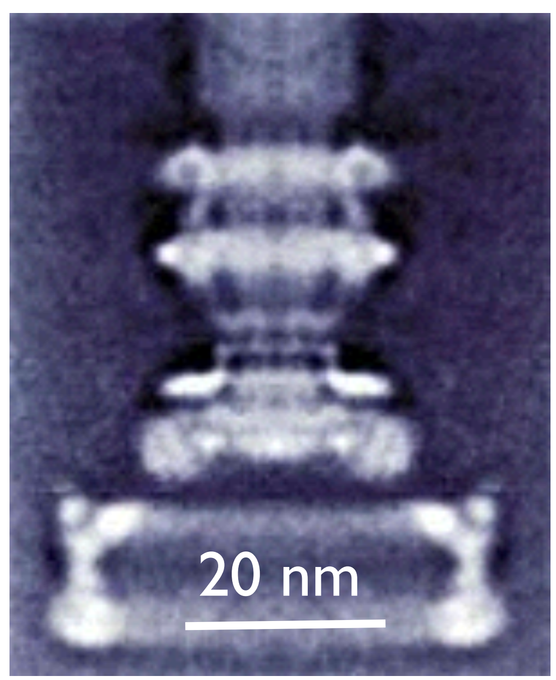

Chen et al (2011) EMBO Journal

Torque-speed relation

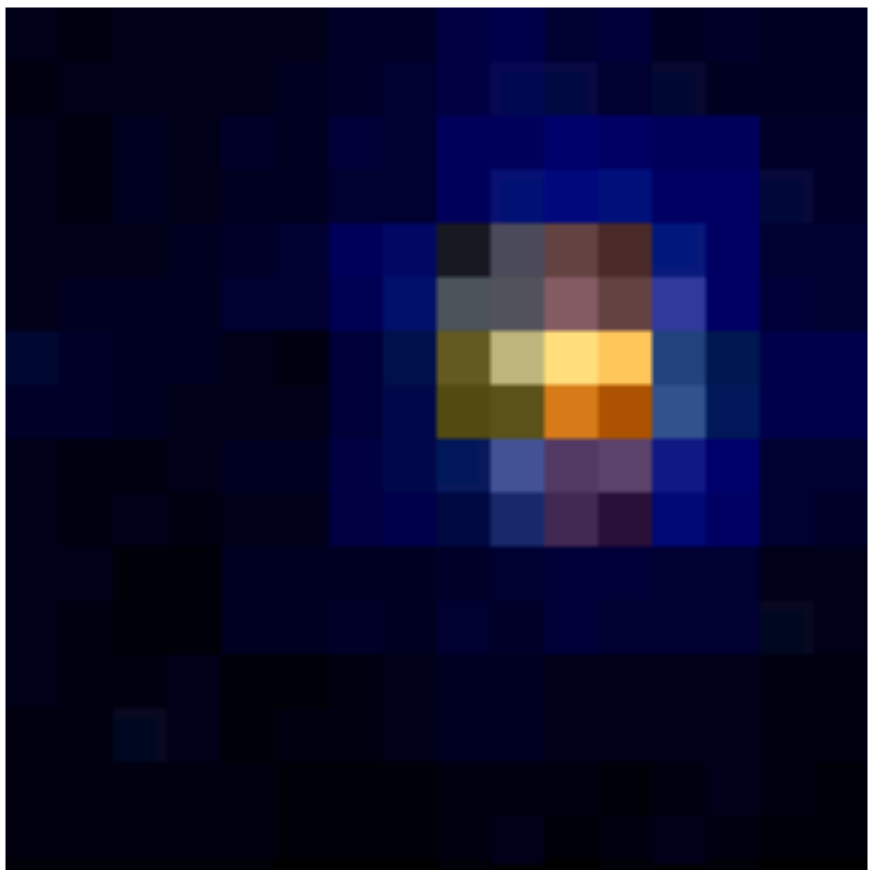

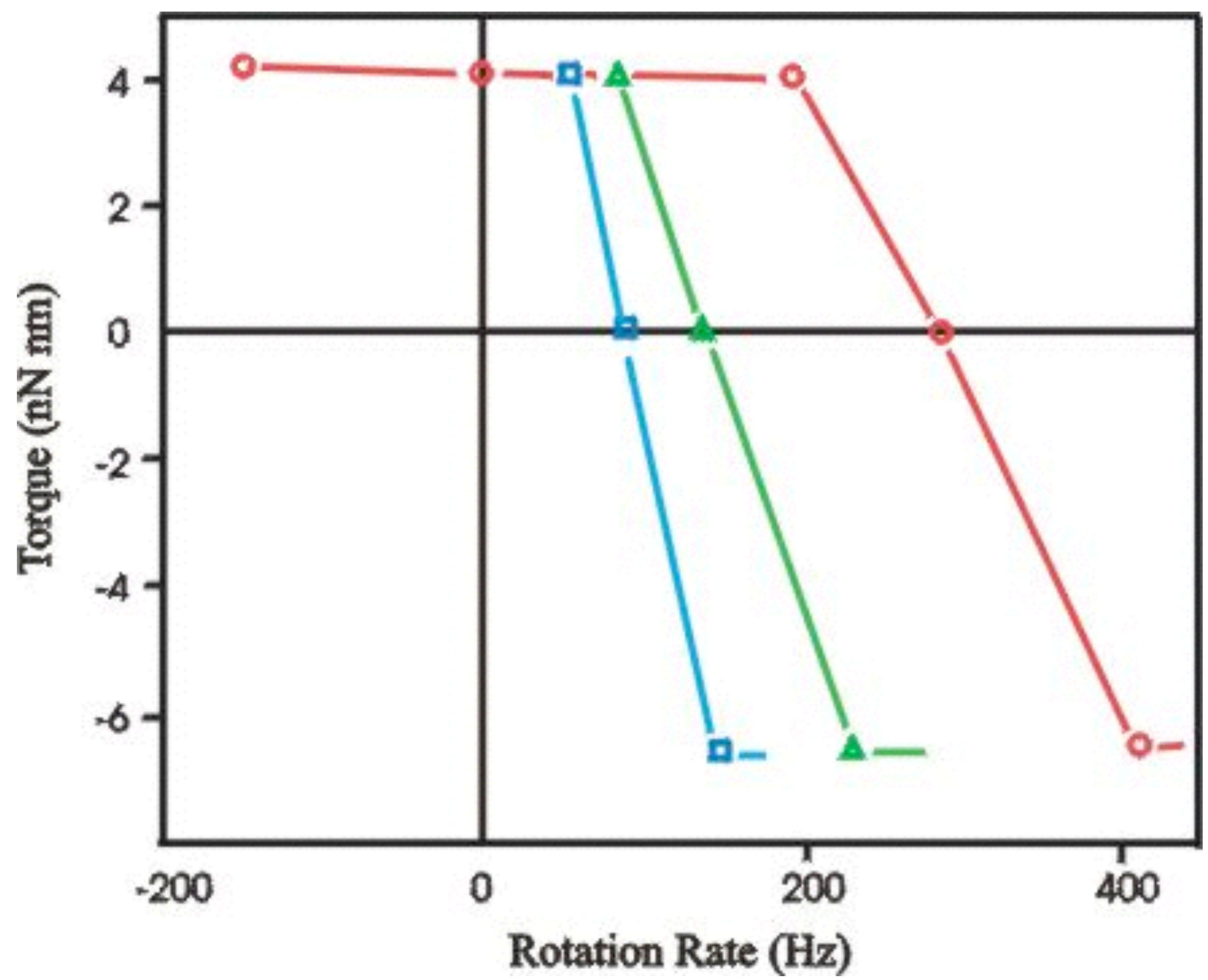

200 nm fluorescent bead attached to a flagellar motor
26 steps per revolution
30x slower than real time
2400 frames per second
position resolution ~5 nm

Berry group, Oxford

Volvox carteri

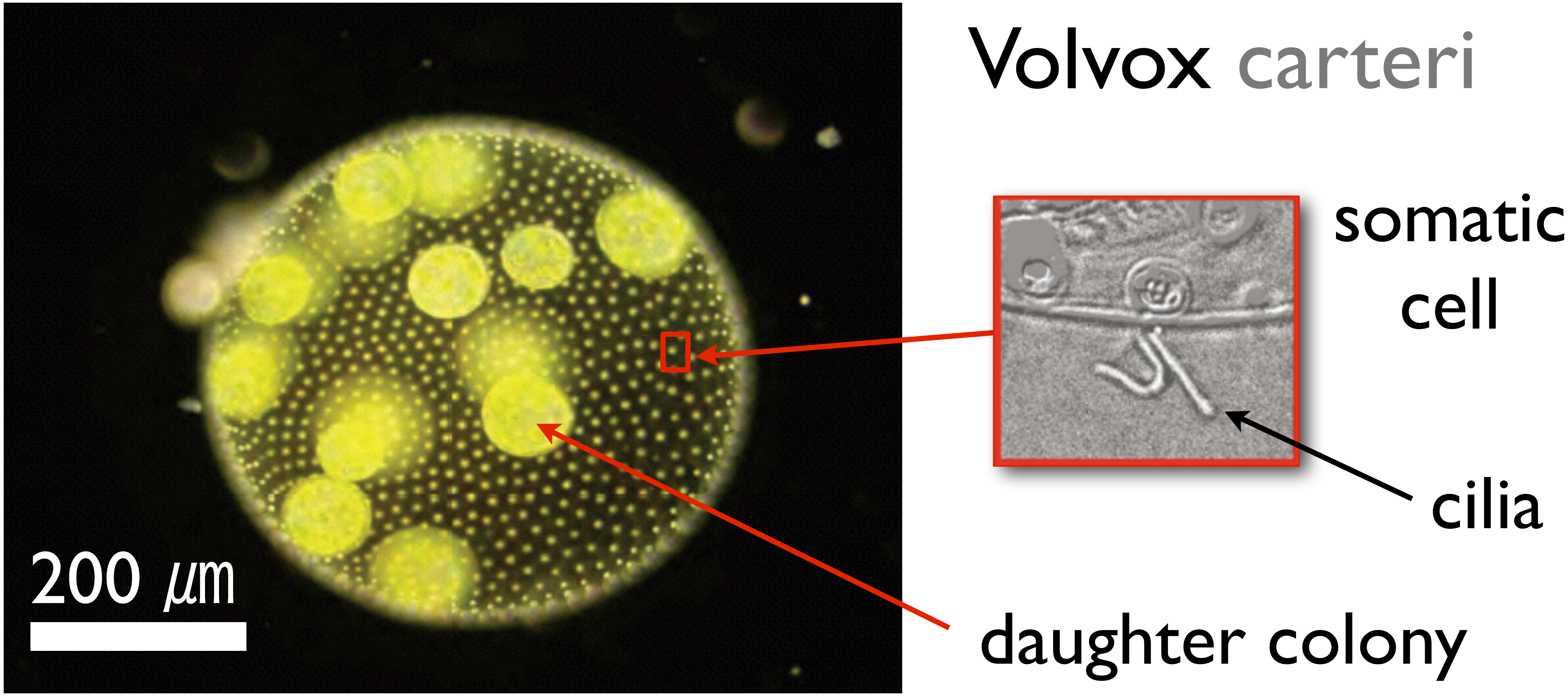

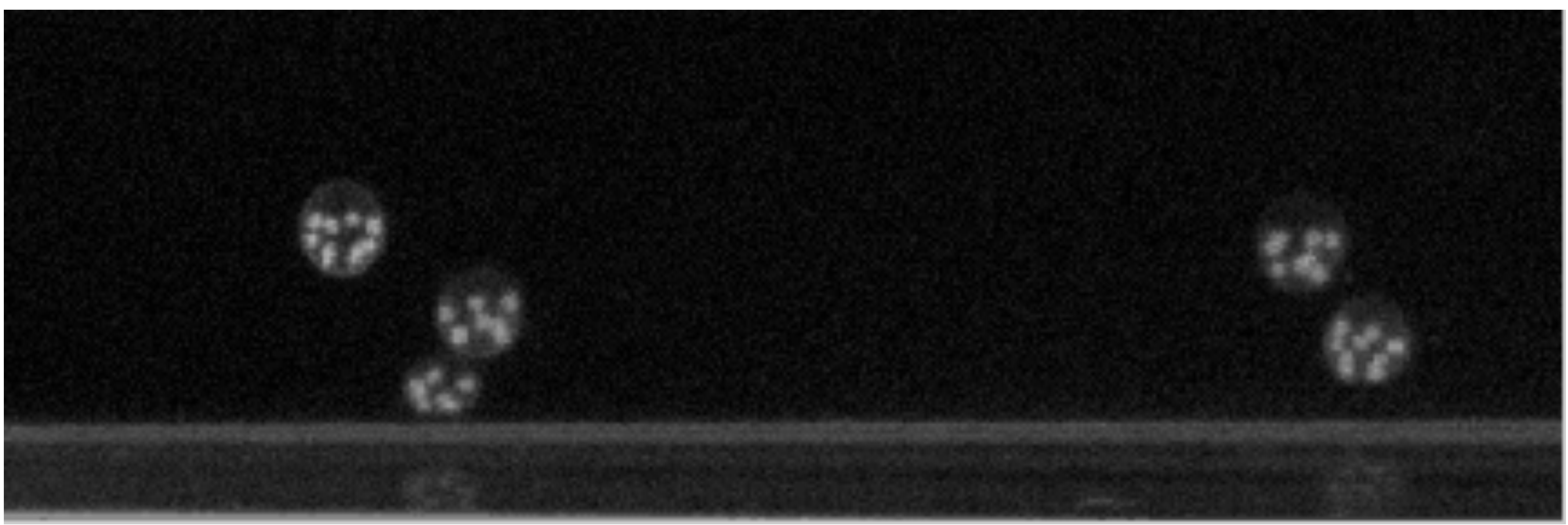

Drescher et al (2010) PRL

dunkel@math.mit.edu

Chlamydomonas alga

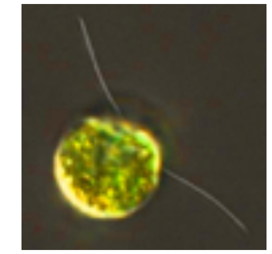

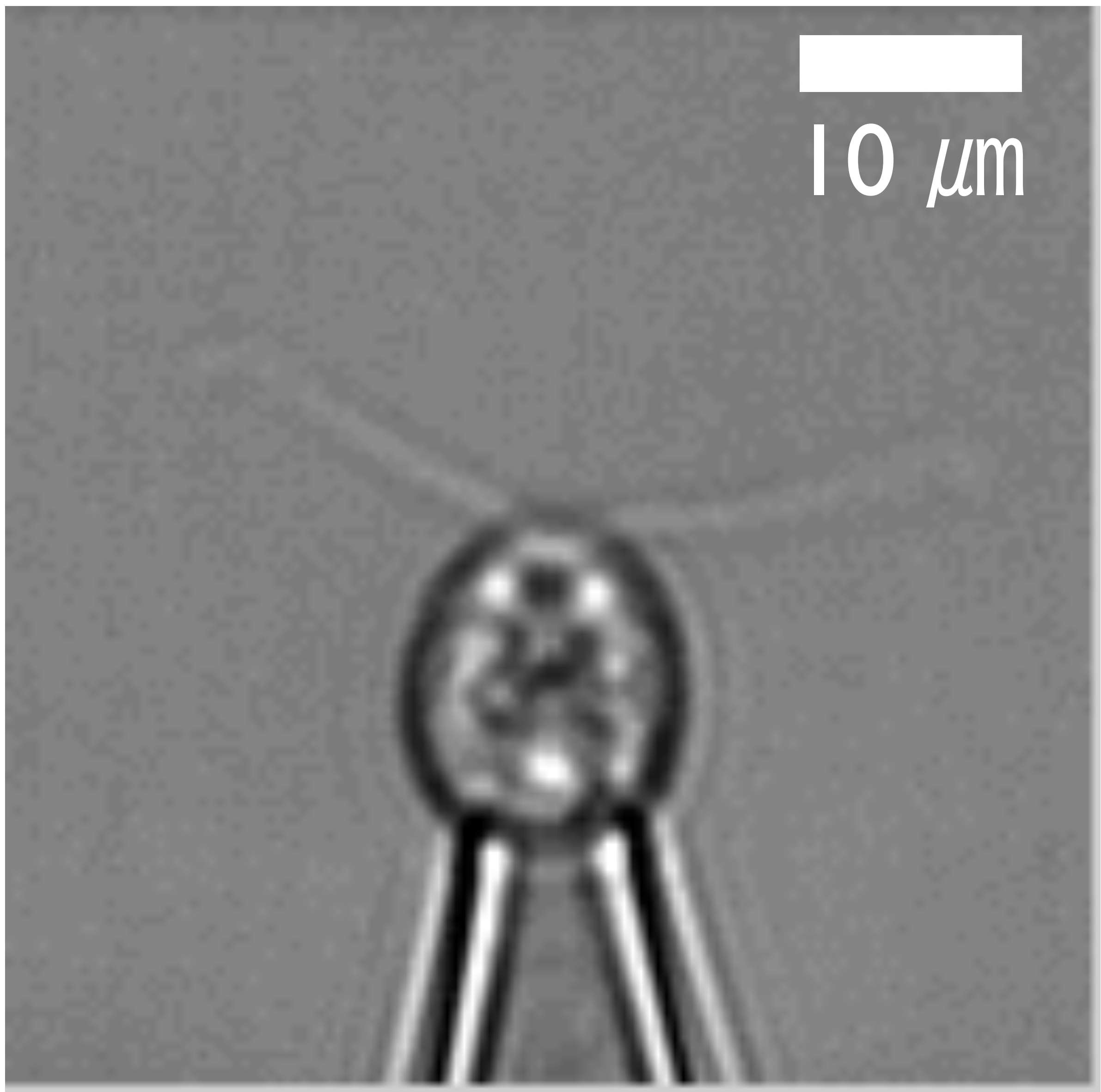

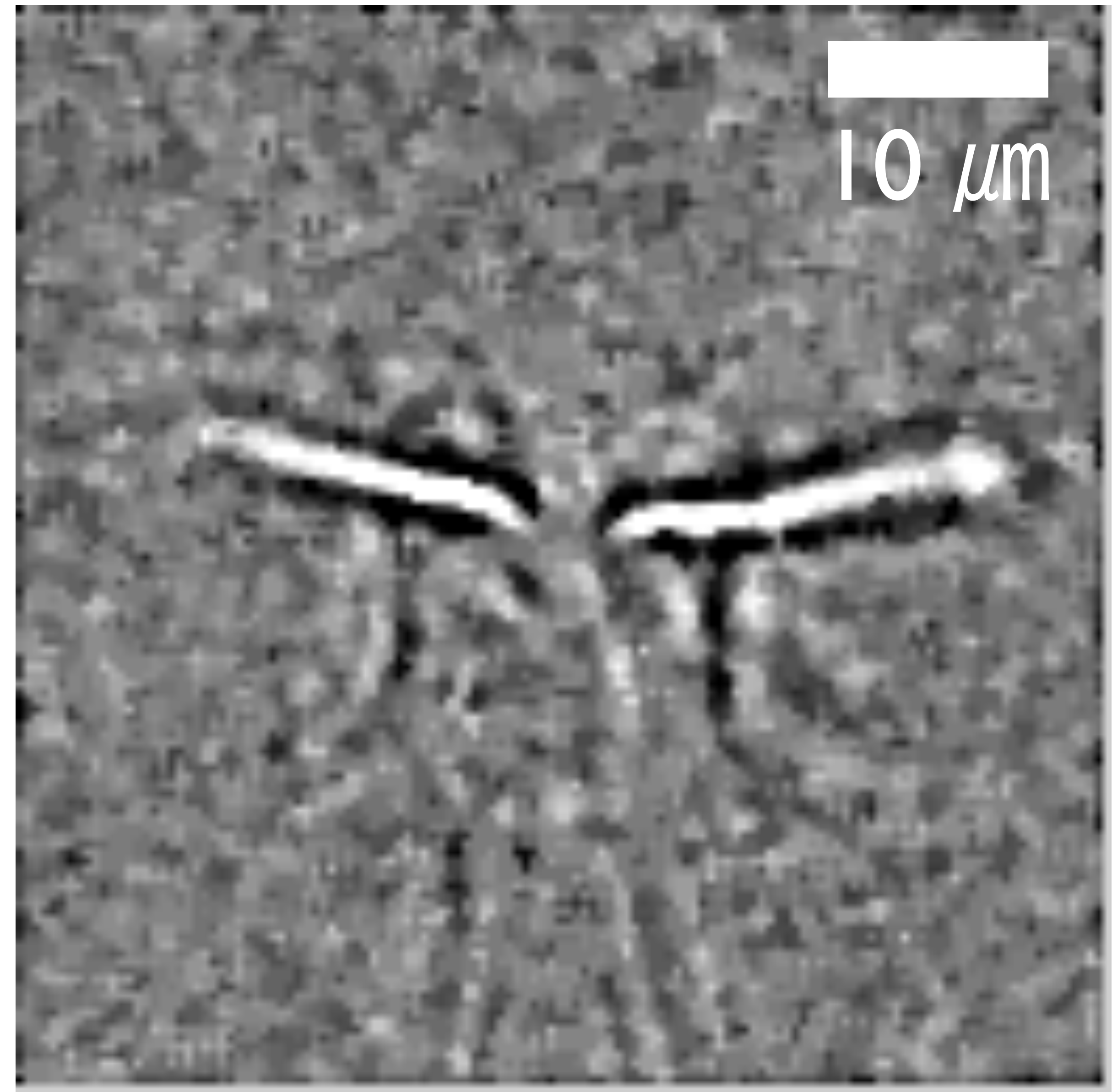

~ 50 beats / sec

speed ~100 μm/s

Goldstein et al (2011) PRL

Chlamy

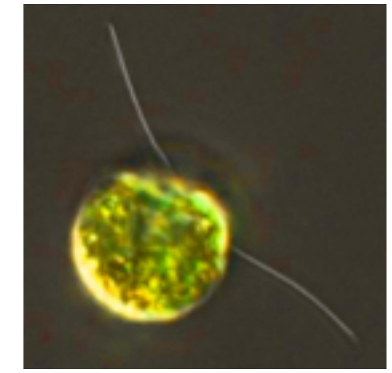

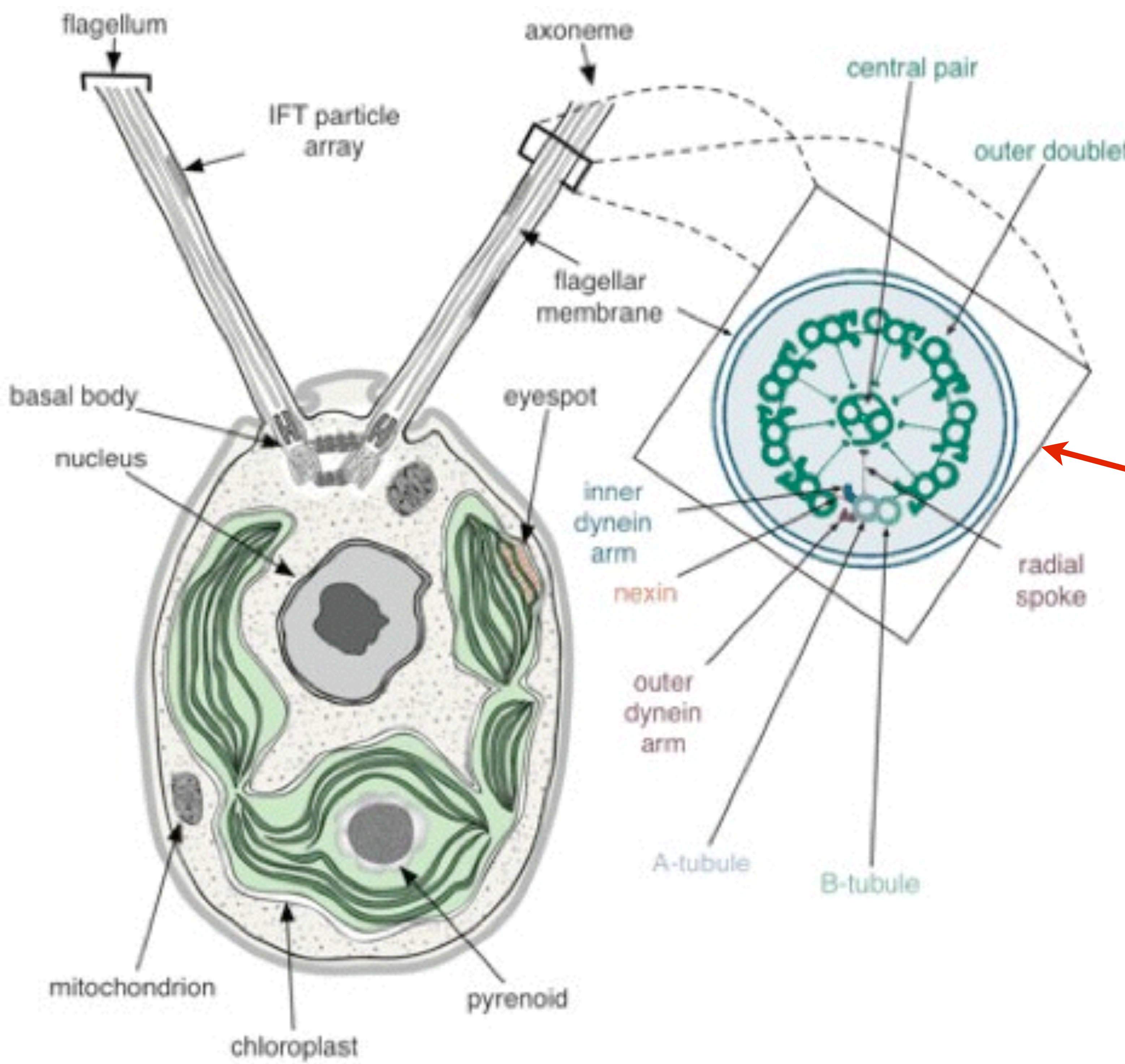

9+2

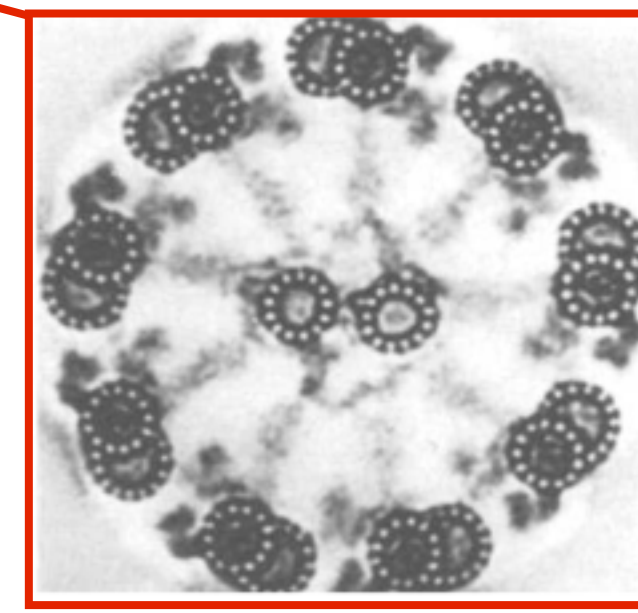

Merchant et al (2007) Science

dunkel@math.mit.edu

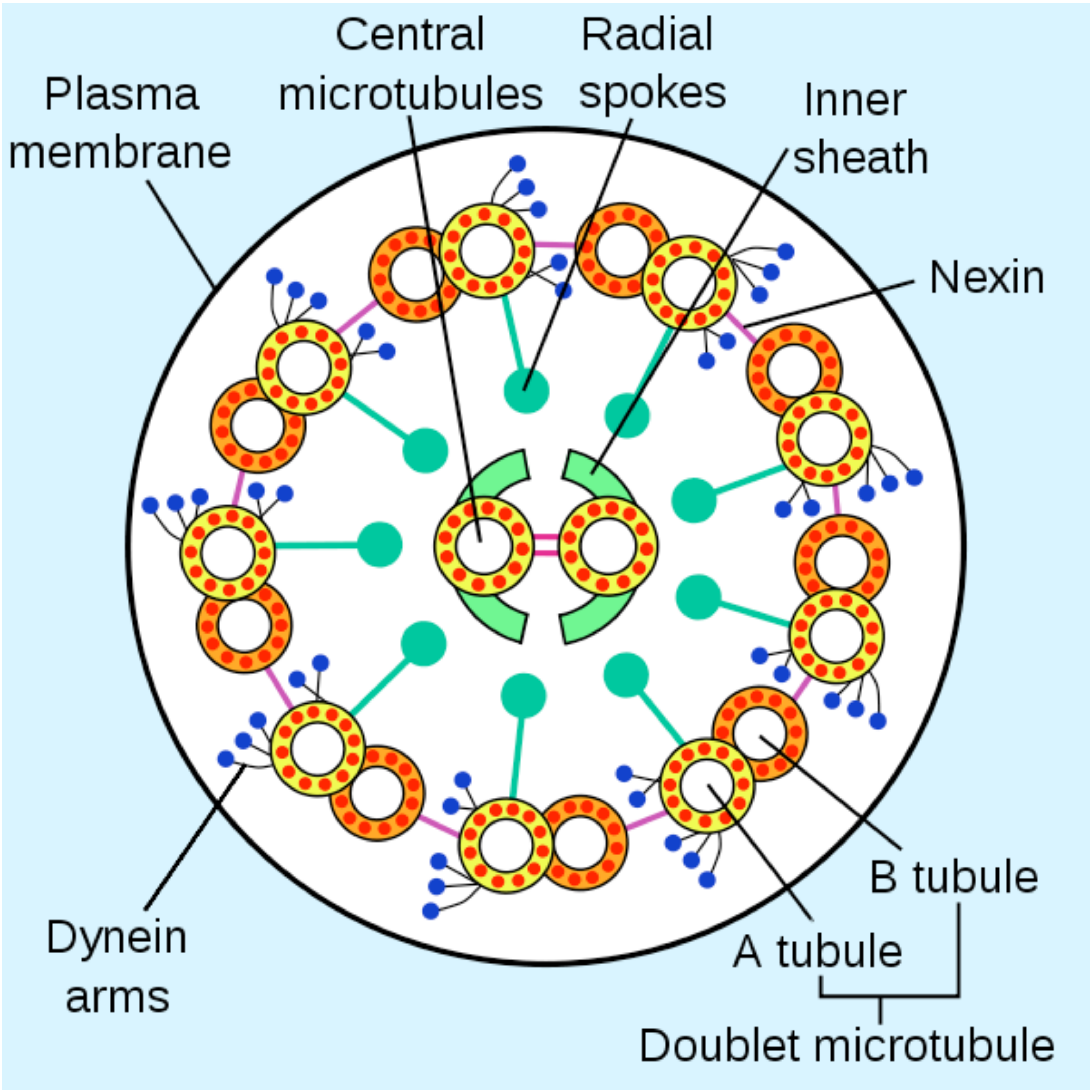

dunkel@math.mit.edu

Eukaryotic motors

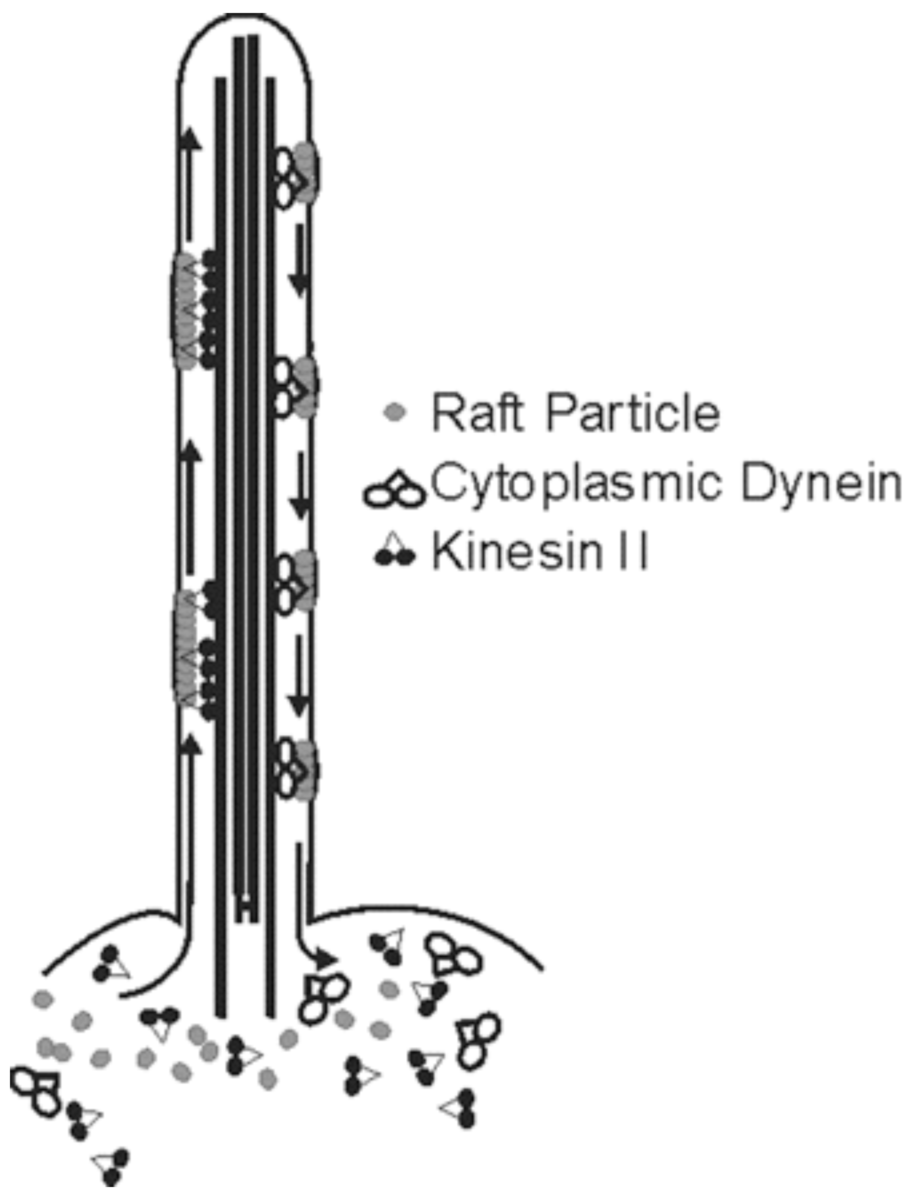

Sketch: dynein molecule carrying cargo down a microtubule

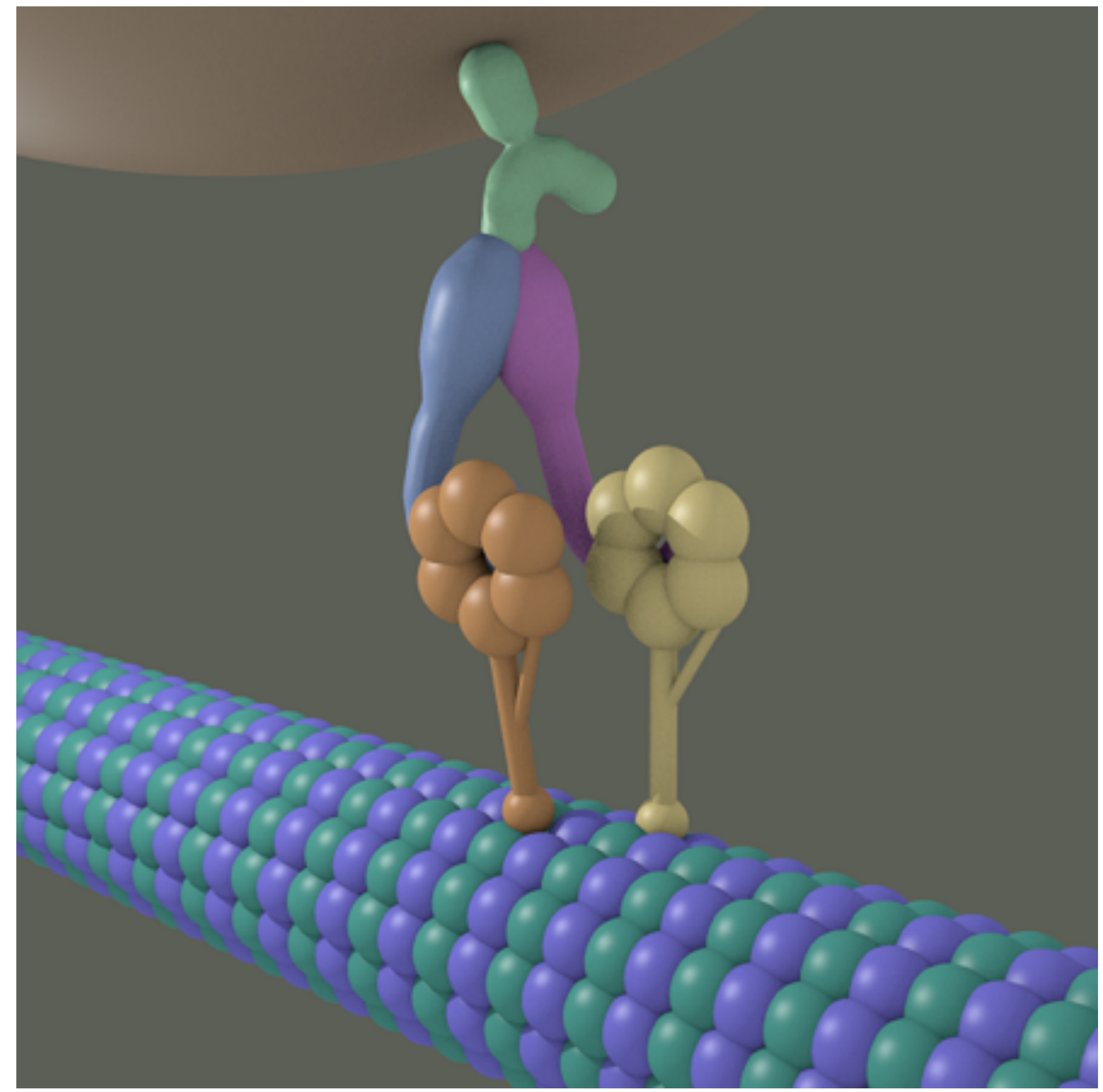

http://www.plantphysiol.org/content/127/4/1500/F4.expansion.html

Yildiz lab, Berkeley

dunkel@math.mit.edu

Microtubule filament “tracks”

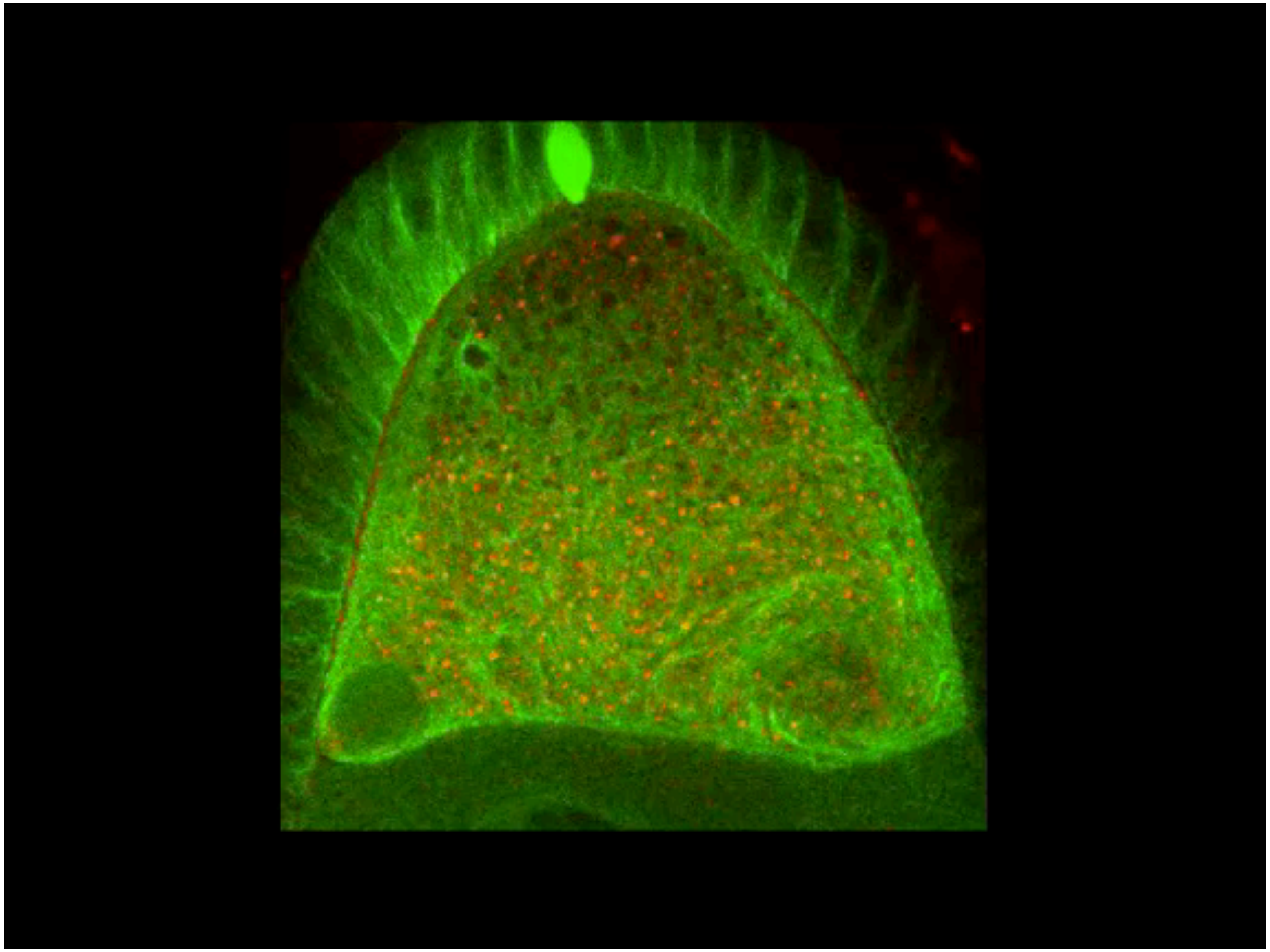

Drosophila oocyte

Physical parameters (e.g. bending rigidity) from fluctuation analysis

dunkel@math.mit.edu

unlike dyneins (most) kinesins walk towards plus end of microtubule

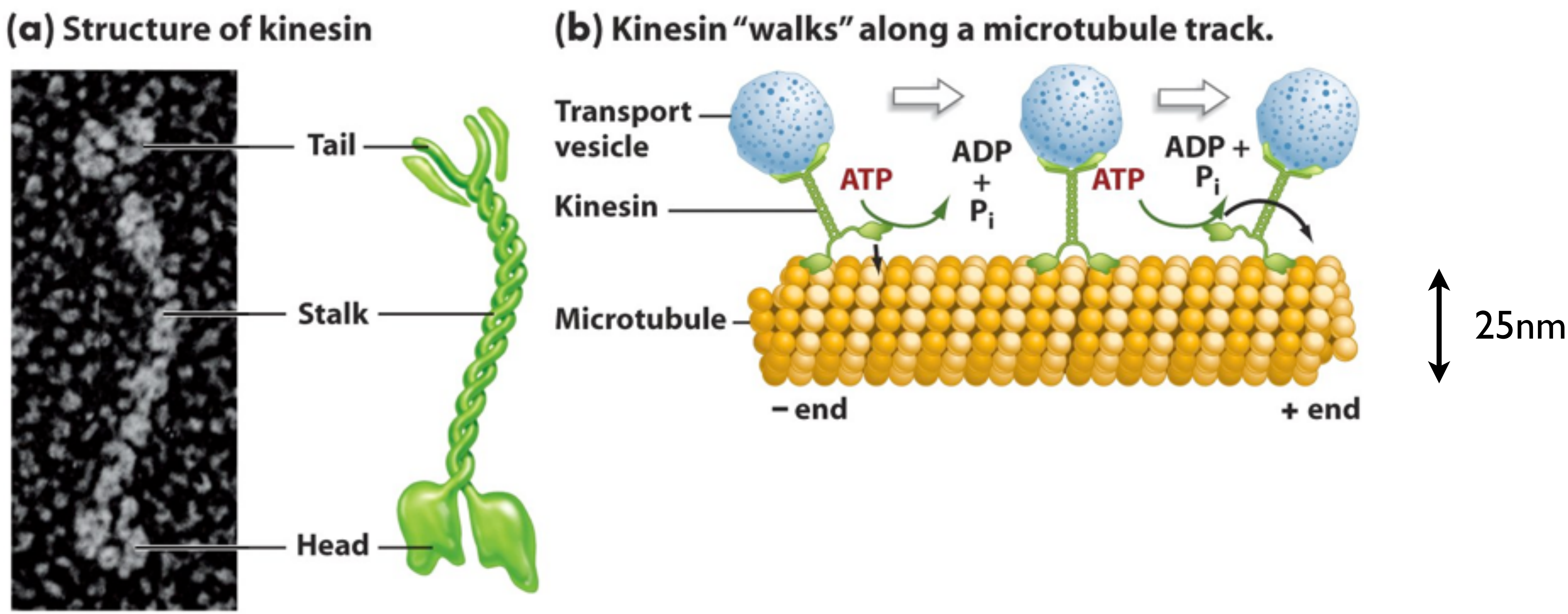

Figure 7-37 Biological Science, 2/e

dunkel@math.mit.edu

Kinesin walks hand-over-hand

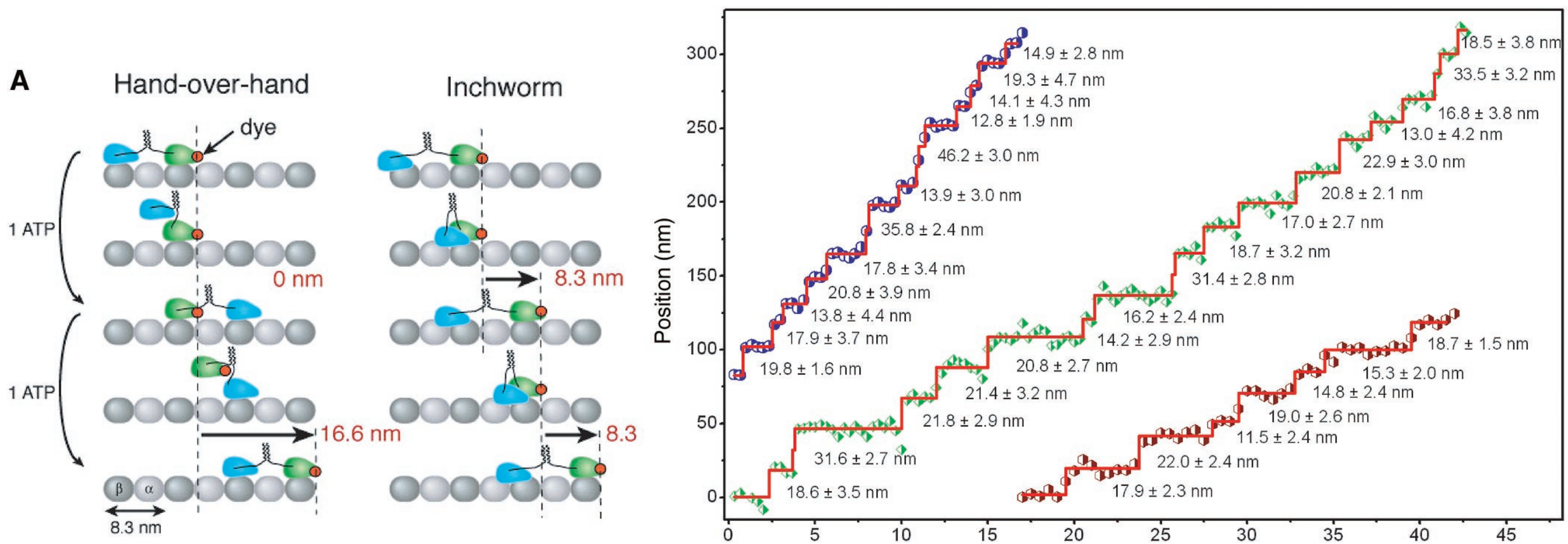

Yildiz et al (2005) Science

Kinesin walks hand-over-hand

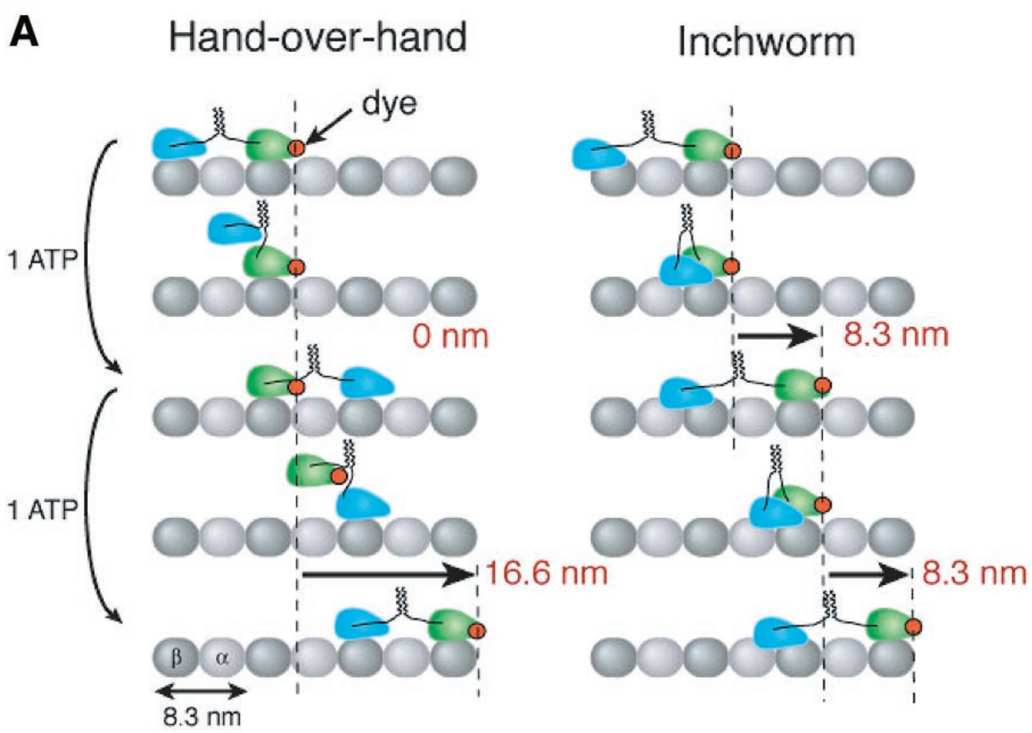

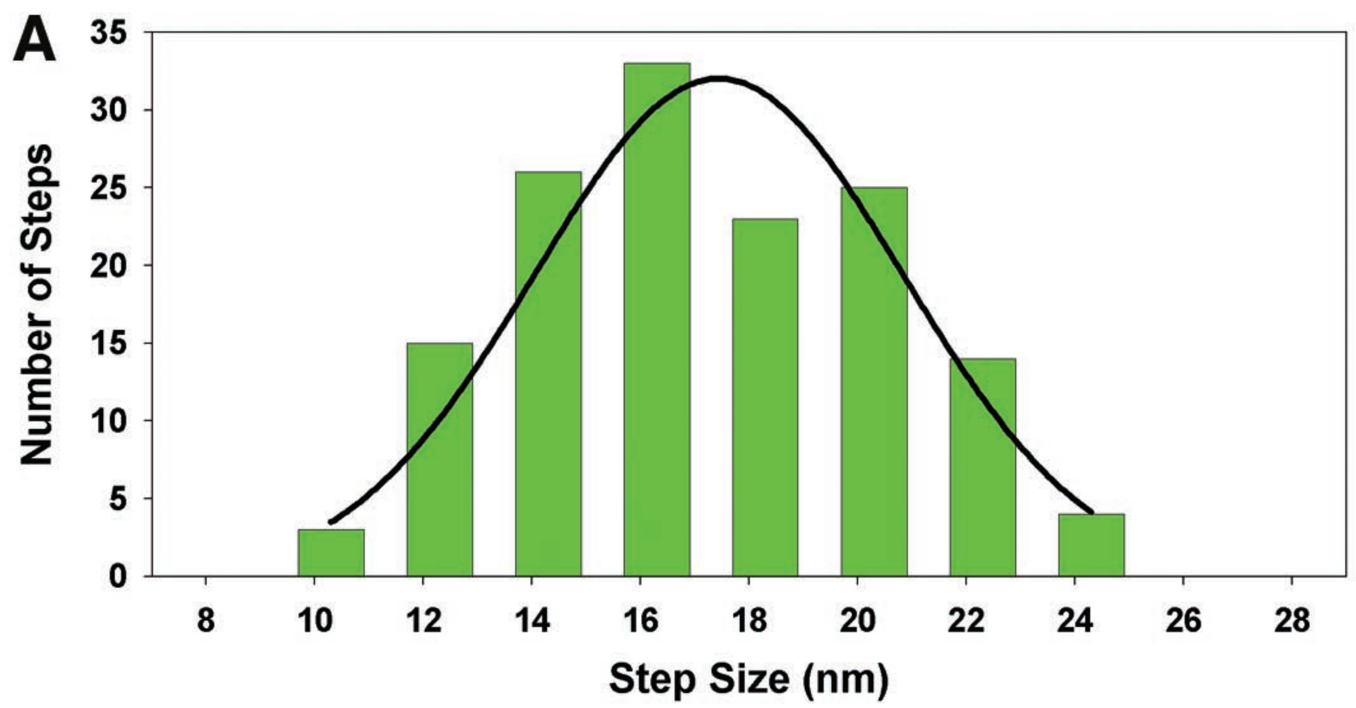

Yildiz et al (2005) Science

dunkel@math.mit.edu

Intracellular transport

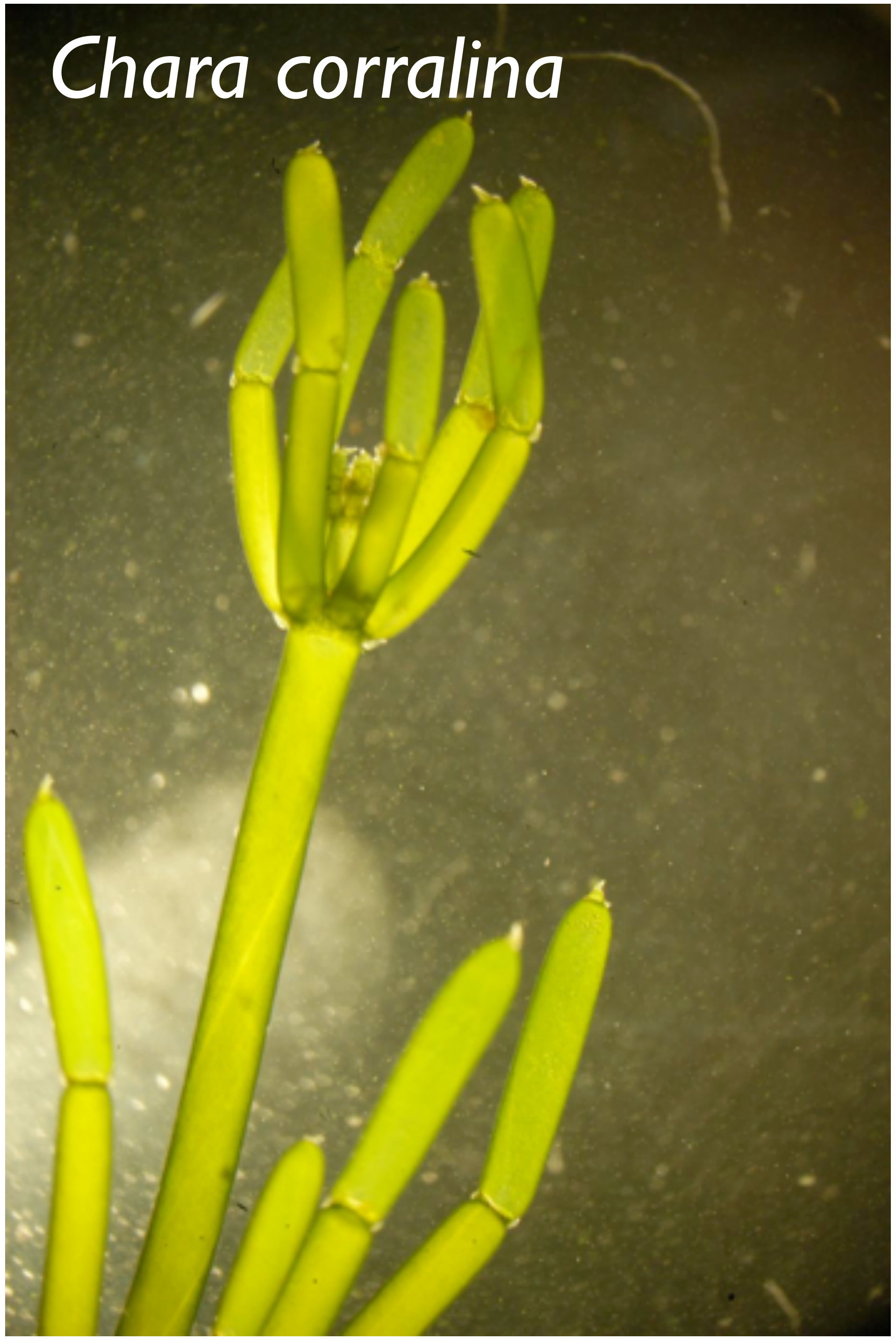

http://damtp.cam.ac.uk/user/gold/movies.html

dunkel@math.mit.edu

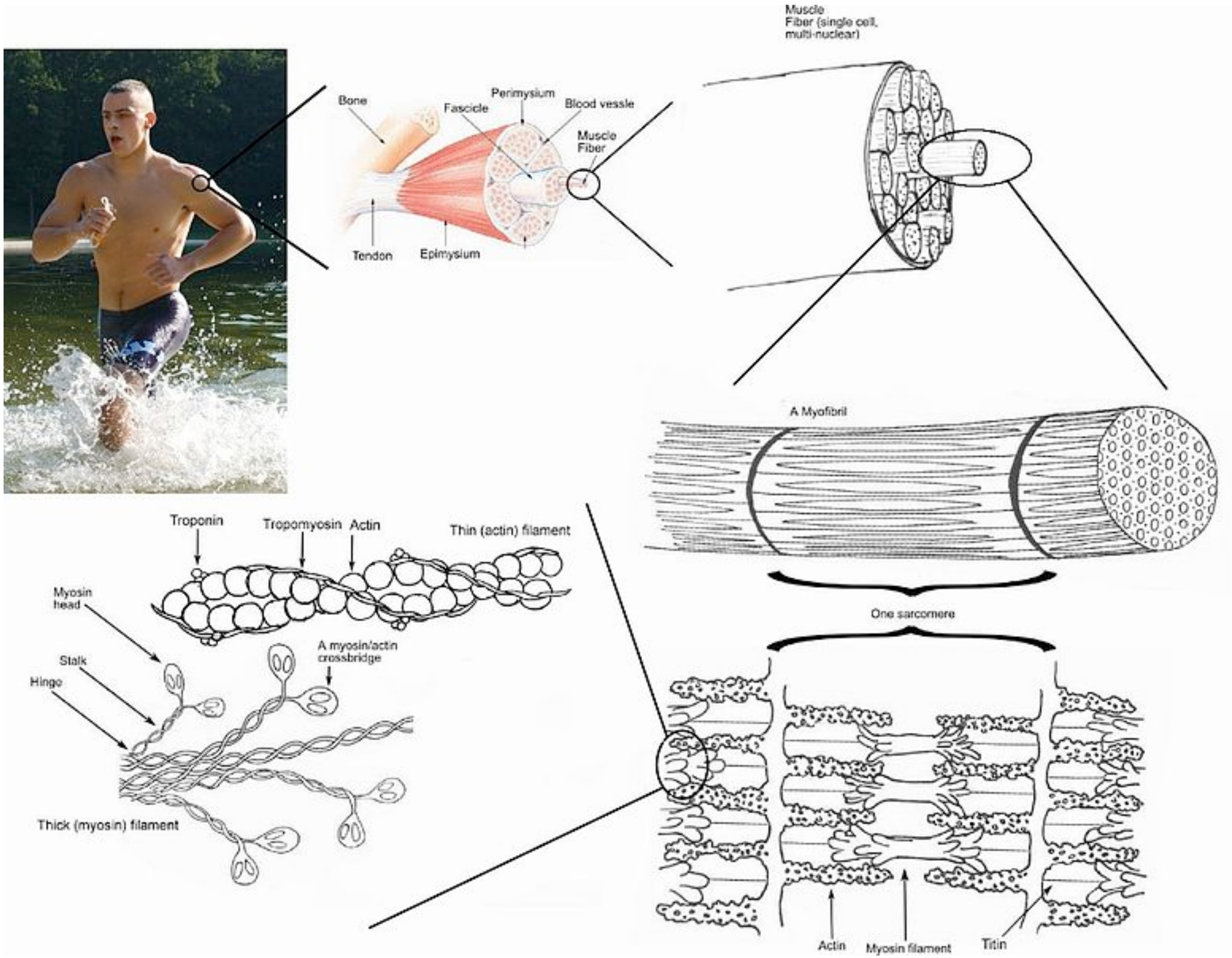

Muscle
Fiber (single cell, multi-nuclear)
Bone
Fascicle
Perimysium
Blood vessle
Muscle
Fiber
Tendon
Epimysium
A Myofibril
One sarcomere
Troponin
Tropomyosin
Actin
Thin (actin) filament
Myosin head
Stalk
Hinge
A myosin/actin crossbridge
Thick (myosin) filament
Actin
Myosin filament
Titin

wiki

Muscular contractions: Actin + Myosin

G-Actin

(globular)

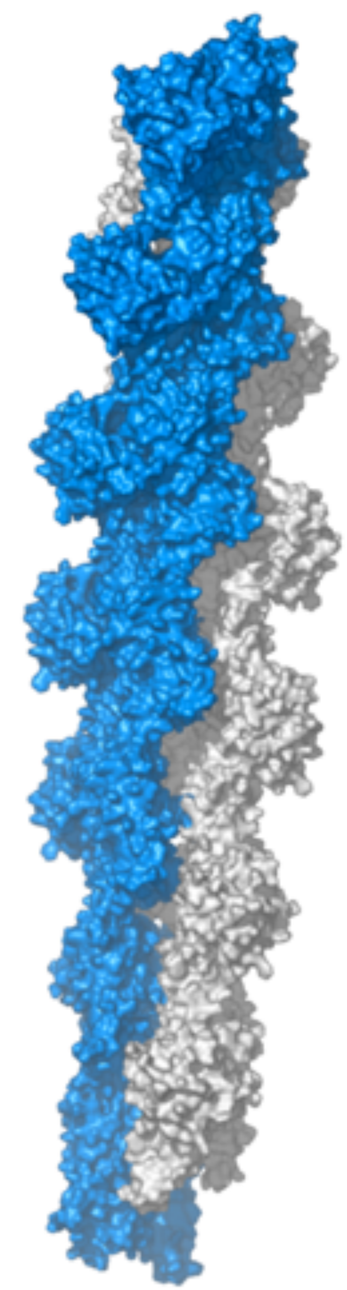

F-Actin

helical filament

dunkel@math.mit.edu

Actin-Myosin

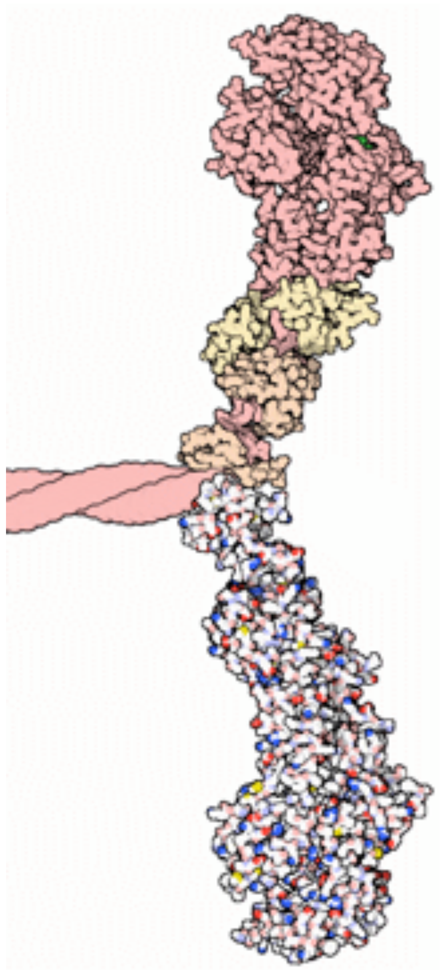

Myosin

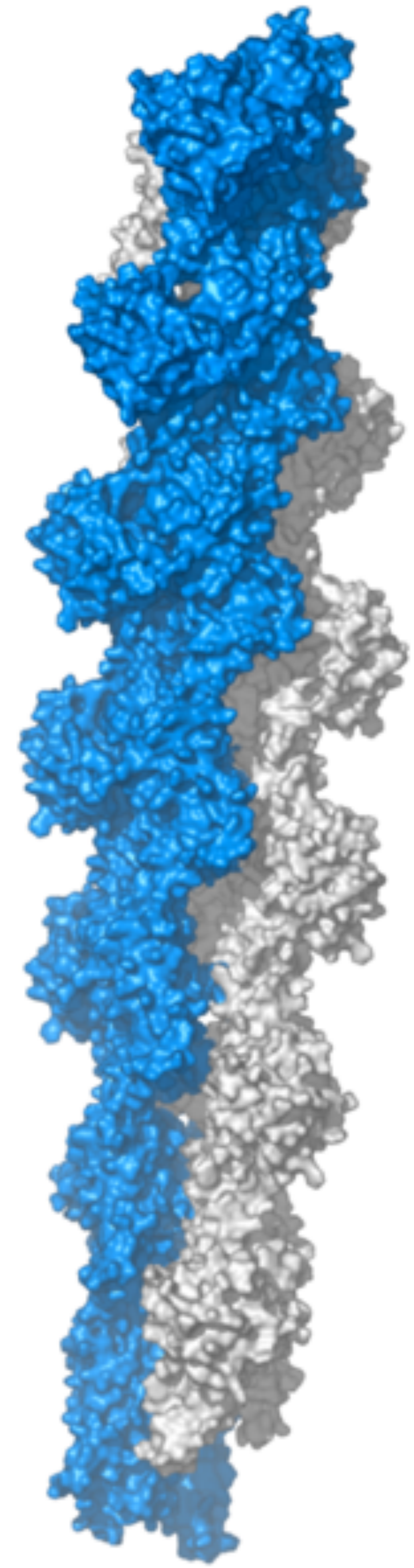

F-Actin

helical filament

Actin-Myosin

Myosin

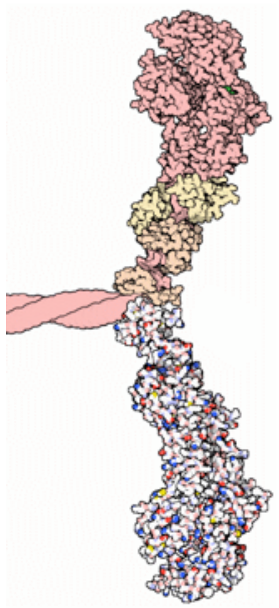

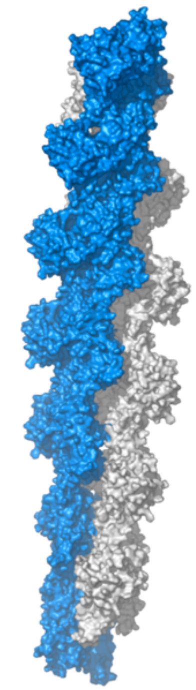

F-Actin

helical filament

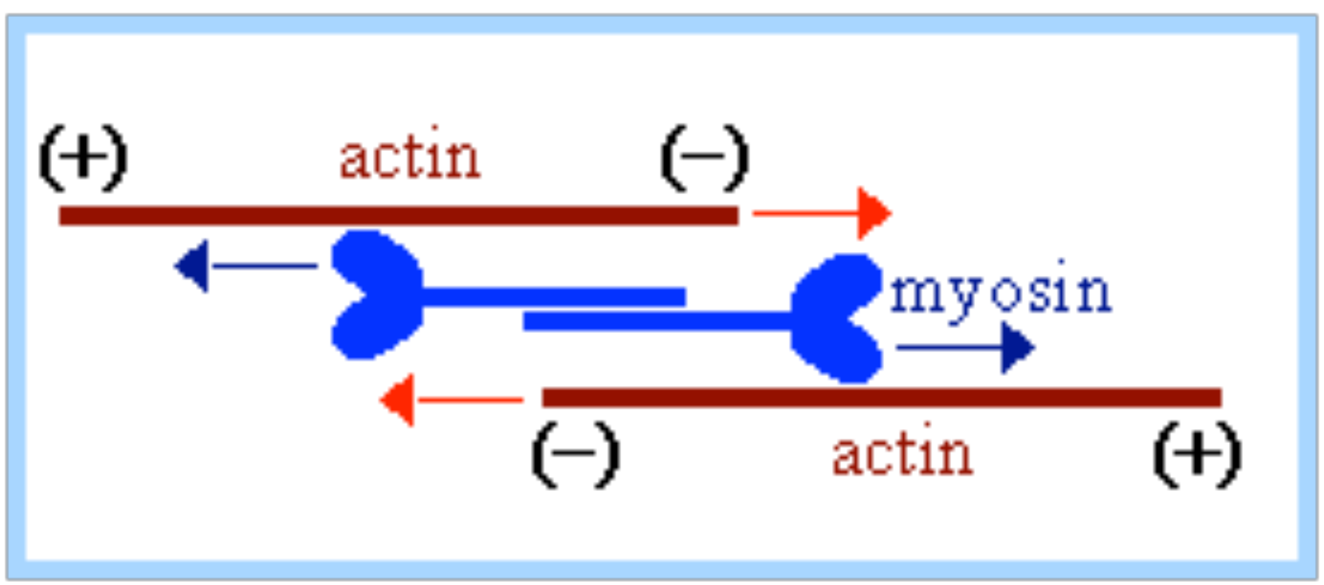

myosin-II

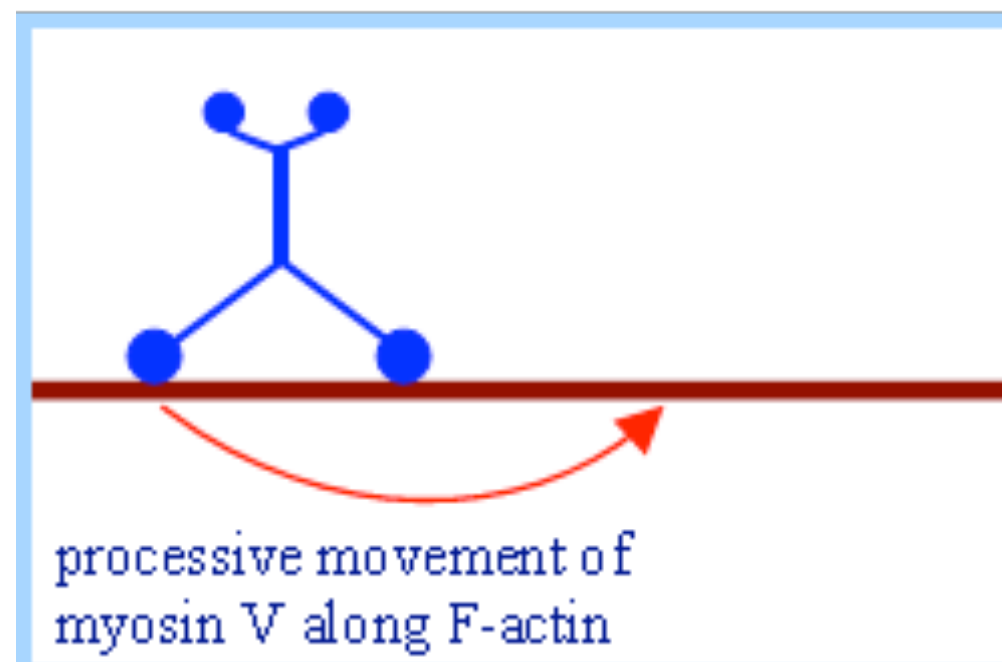

myosin-V

dunkel@math.mit.edu

Myosin walks hand-over-hand

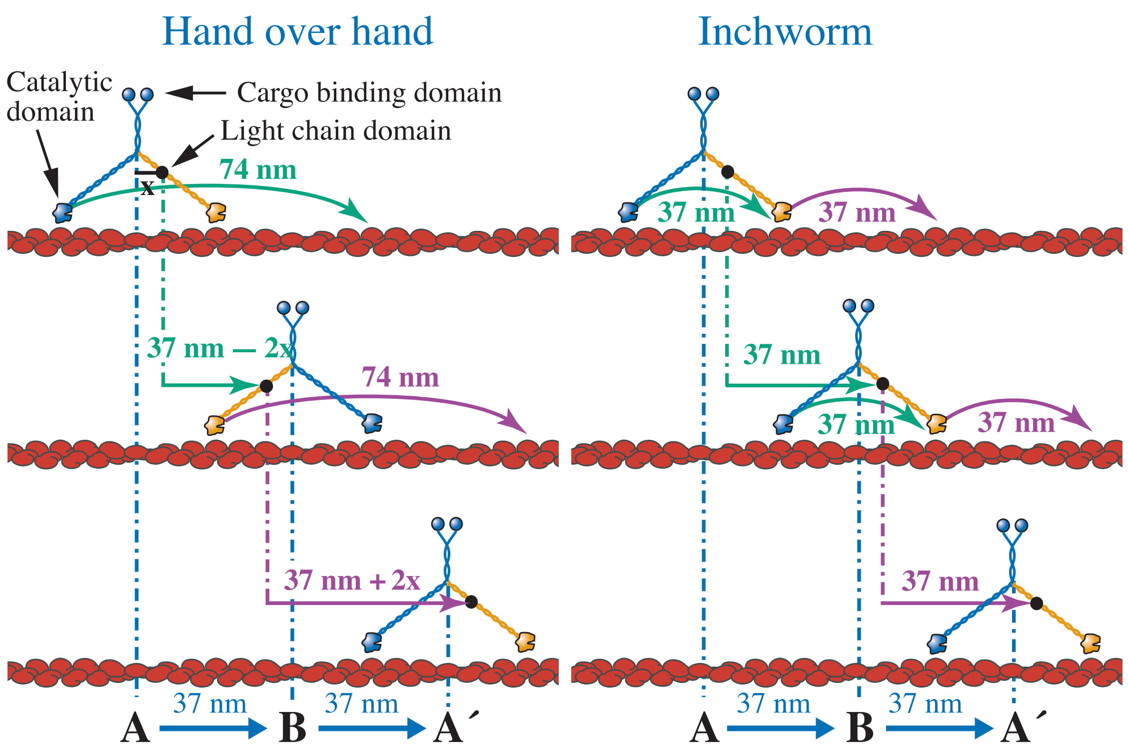

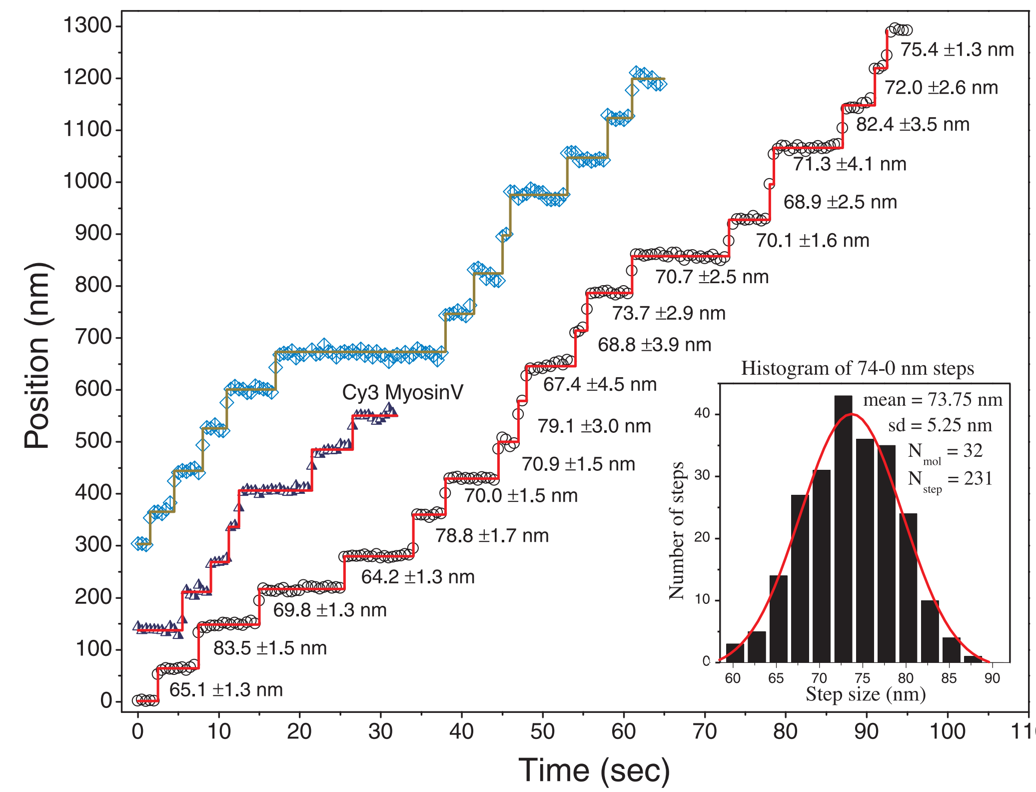

Fig. 3. Stepping traces of three different myosin V molecules displaying 74-nm steps and histogram (inset) of a total of 32 myosin V's taking 231 steps. Calculation of the standard deviation of step sizes can be found (*14*). Traces are for BR-labeled myosin V unless noted as Cy3 Myosin V. Lower right trace, see Movie S1.

Yildiz et al (2003) Science

dunkel@math.mit.edu

Bacteria-driven motor

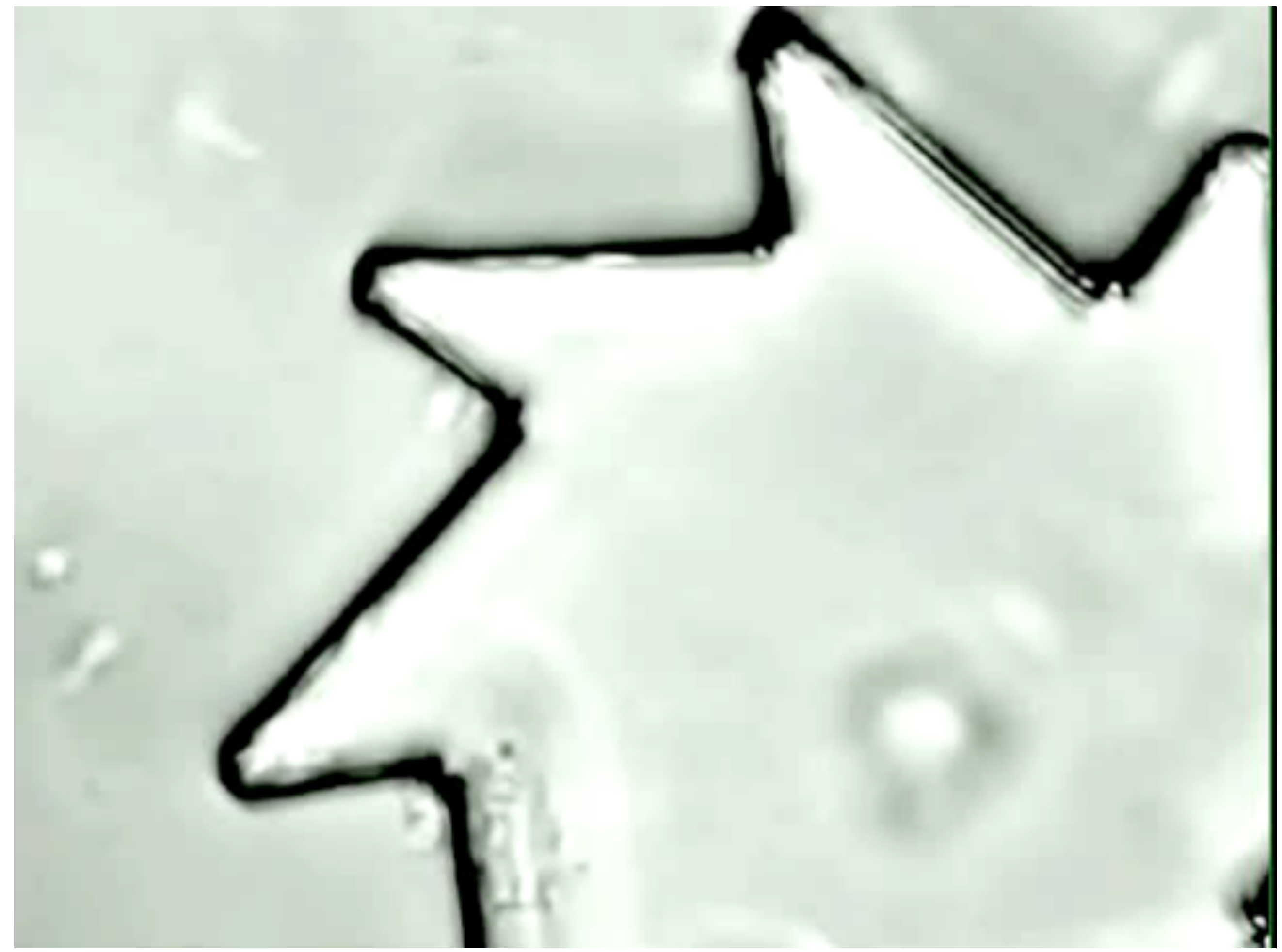

Di Leonardo (2010) PNAS

dunkel@math.mit.edu

Feynman-Smoluchowski ratchet

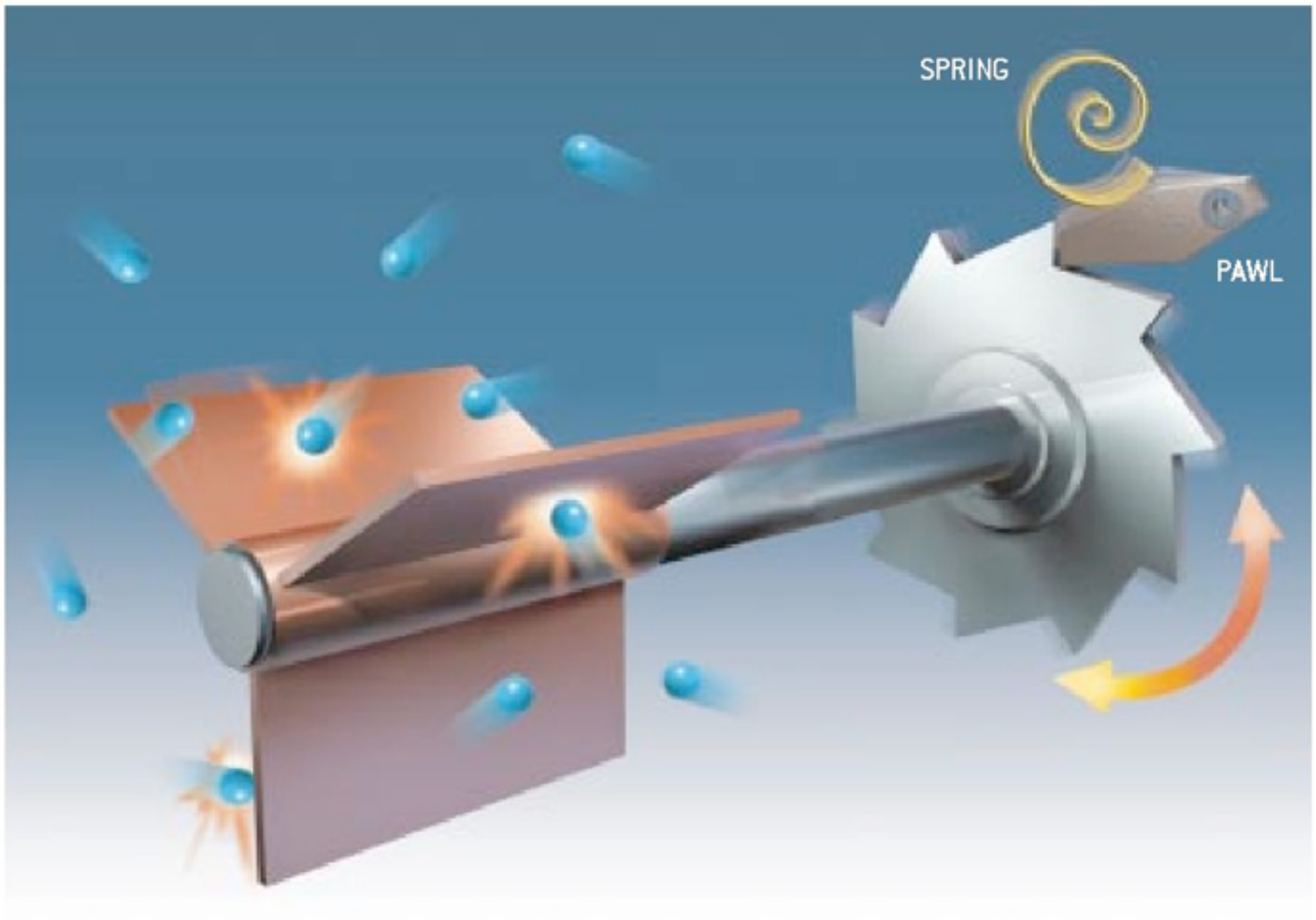

generic model of a micro-motor

dunkel@math.mit.edu

Basic ingredients for rectification

- some form of noise (not necessarily thermal)
- some form of nonlinear interaction potential
- spatial symmetry breaking
- non-equilibrium (broken detailed balance) due to presence of external bias, energy input, periodic forcing, memory, etc.

dunkel@math.mit.edu

Eukaryotic motors

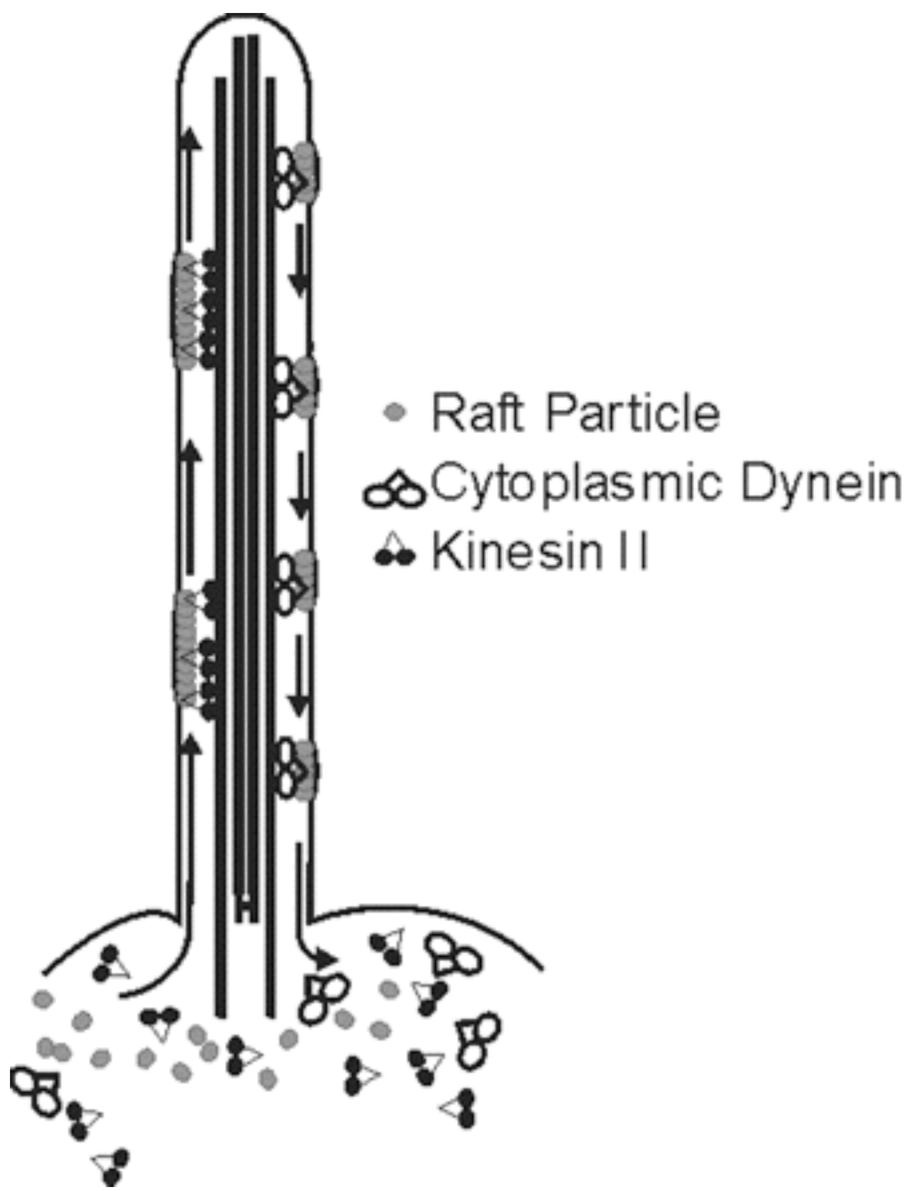

http://www.plantphysiol.org/content/127/4/1500/F4.expansion.html

Sketch: dynein molecule carrying cargo down a microtubule

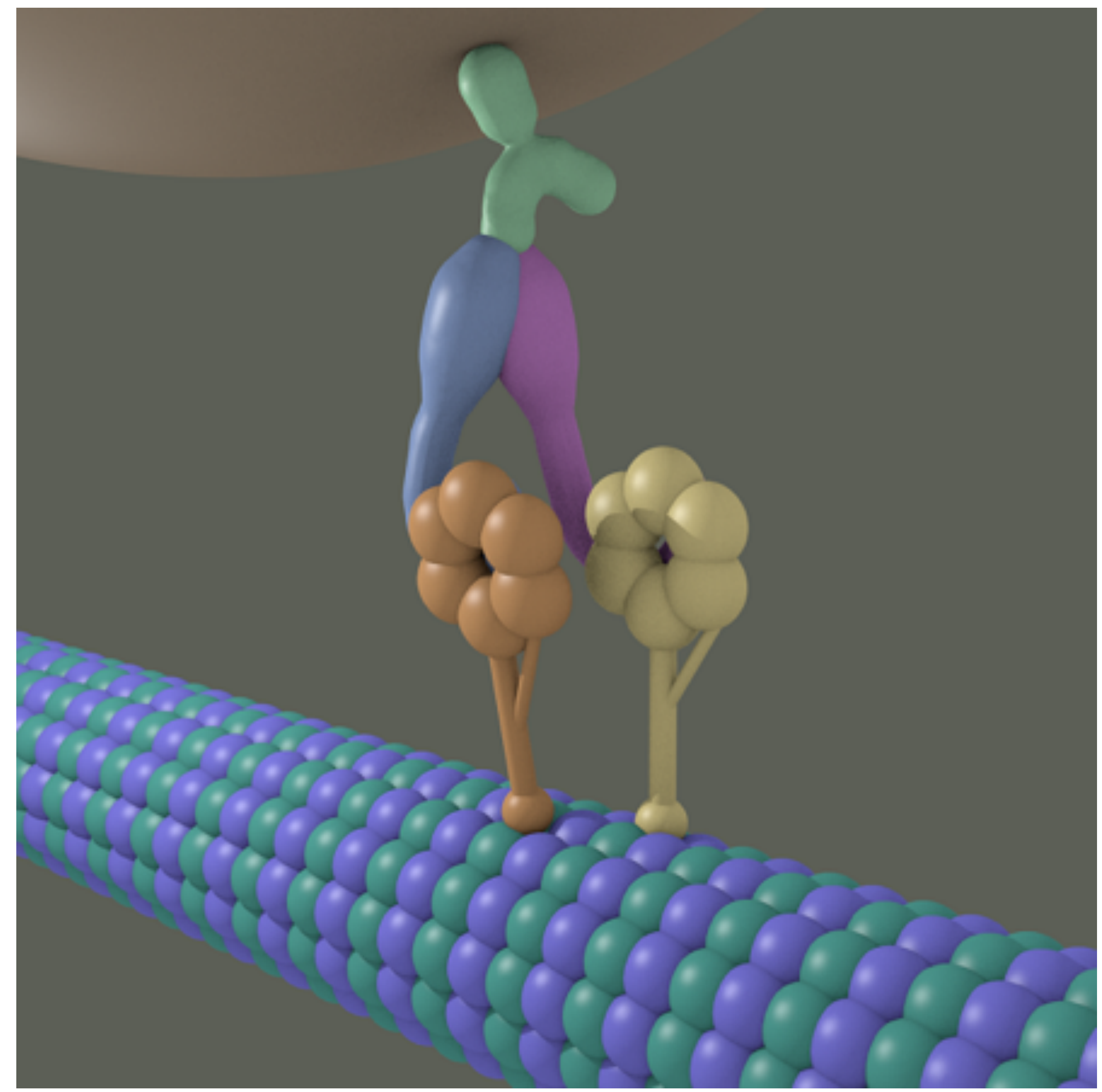

Yildiz lab, Berkeley

dunkel@math.mit.edu

Most biological micro-motors operate in the low Reynolds number regime, where inertia is negligible. A minimal model can therefore be formulated in terms of an over-damped Ito-SDE

$$dX(t) = -U'(X)\, dt + F(t)dt + \sqrt{2D(t)} * dB(t). \tag{1.116}$$

Most biological micro-motors operate in the low Reynolds number regime, where inertia is negligible. A minimal model can therefore be formulated in terms of an over-damped Ito-SDE

$$dX(t) = -U'(X)\,dt + F(t)dt + \sqrt{2D(t)} * dB(t). \tag{1.116}$$

Here, U is a periodic potential

$$U(x) = U(x + L) \tag{1.117a}$$

with broken reflection symmetry, i.e., there is no δx such that

$$U(-x) = U(x + \delta x). \tag{1.117b}$$

Most biological micro-motors operate in the low Reynolds number regime, where inertia is negligible. A minimal model can therefore be formulated in terms of an over-damped Ito-SDE

$$dX(t) = -U'(X)\, dt + F(t)dt + \sqrt{2D(t)} * dB(t). \tag{1.116}$$

Here, U is a periodic potential

$$U(x) = U(x + L) \tag{1.117a}$$

with broken reflection symmetry, i.e., there is no δx such that

$$U(-x) = U(x + \delta x). \tag{1.117b}$$

A typical example is

$$U = U_0[\sin(2\pi x/L) + \frac{1}{4}\sin(4\pi x/L)]. \tag{1.117c}$$

The function $F(t)$ is a deterministic driving force, and the noise amplitude $D(t)$ can be time-dependent as well.

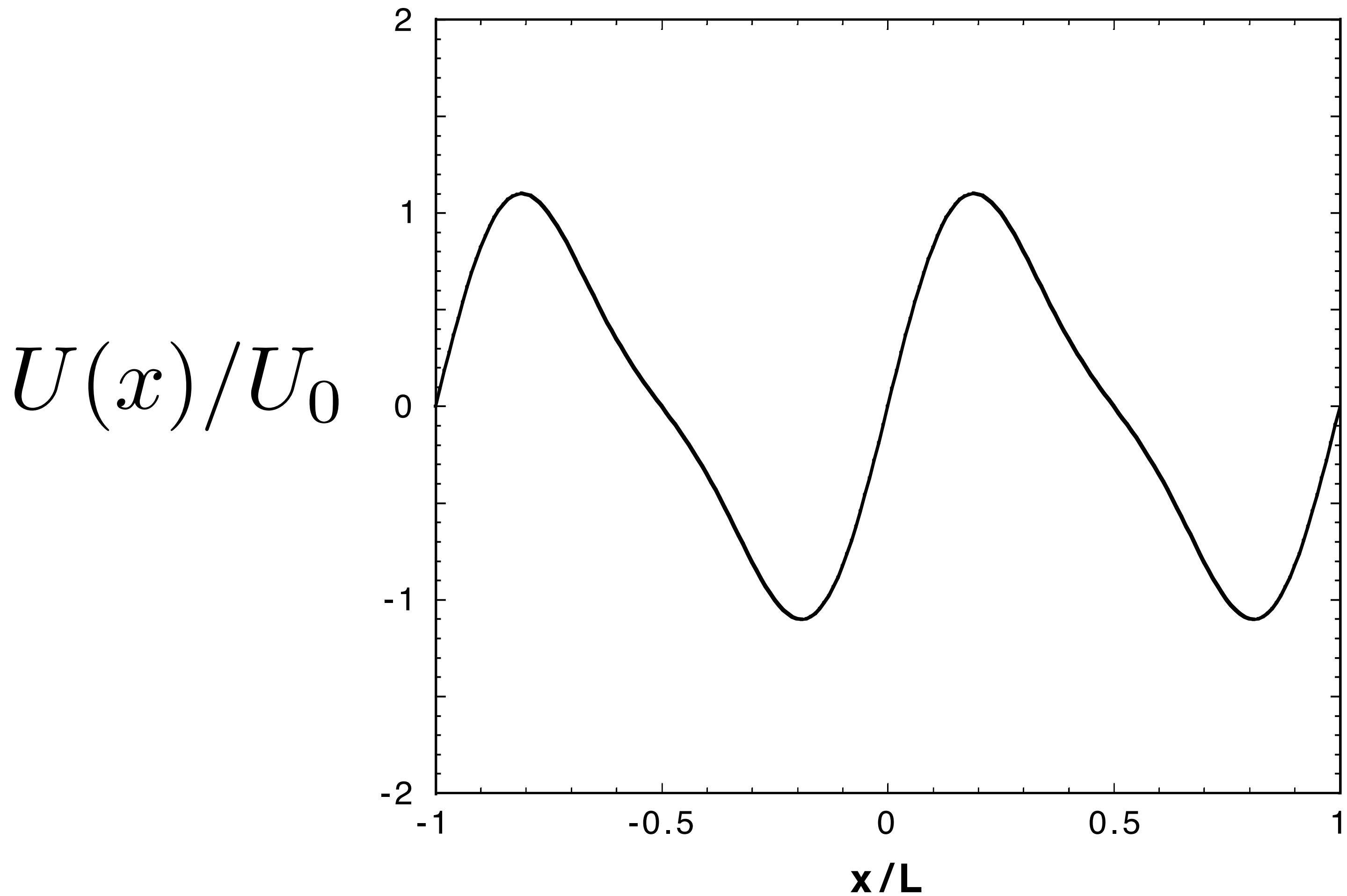

Fig. 2.2. Typical example of a ratchet-potential $V(x)$, periodic in space with period L and with broken spatial symmetry. Plotted is the example from (2.3) in dimensionless units.

The corresponding FPE for the associated PDF $p(t, x)$ reads

$$\partial_t p = -\partial_x j \ , \qquad j(t, x) = -\{[U' - F(t)]p + D(t)\partial_x p\}, \tag{1.118}$$

and we assume that p is normalized to the total number of particles, i.e.

$$N_L(t) = \int_0^L dx \, p(t, x) \tag{1.119}$$

gives the number of particles in $[0, L]$. The quantity of interest is the mean particle velocity v_L per period defined by

$$v_L(t) := \frac{1}{N_L(t)} \int_0^L dx \, j(t, x). \tag{1.120}$$

The corresponding FPE for the associated PDF $p(t,x)$ reads

$$\partial_t p = -\partial_x j \ , \qquad j(t,x) = -\{[U' - F(t)]p + D(t)\partial_x p\}, \tag{1.118}$$

and we assume that p is normalized to the total number of particles, i.e.

$$N_L(t) = \int_0^L dx\, p(t,x) \tag{1.119}$$

gives the number of particles in $[0, L]$. The quantity of interest is the mean particle velocity v_L per period defined by

$$v_L(t) := \frac{1}{N_L(t)} \int_0^L dx\, j(t,x). \tag{1.120}$$

Inserting the expression for j, we find for spatially periodic solutions with $p(t,x) = p(t, x+L)$ that

$$v_L = \frac{1}{N_L(t)} \int_0^L dx\, [F(t) - U'(x)]\, p(t,x). \tag{1.121}$$

1.6.1 Tilted Smoluchowski-Feynman ratchet

As a first example, assume that $F = const.$ and $D = const.$ This case can be considered as a (very) simple model for kinesin or dynein walking along a polar microtubule, with the constant force $F \geq 0$ accounting for the polarity. We would like to determine the mean transport velocity v_L for this model.

To evaluate Eq. (1.121), we focus on the long-time limit, noting that a stationary solution $p_\infty(x)$ of the corresponding FPE (1.118) must yield a constant current-density j_∞, i.e.,

$$j_\infty = -[(\partial_x \Phi) p_\infty + D \partial_x p_\infty] \tag{1.122}$$

where

$$\Phi(x) = U(x) - xF \tag{1.123}$$

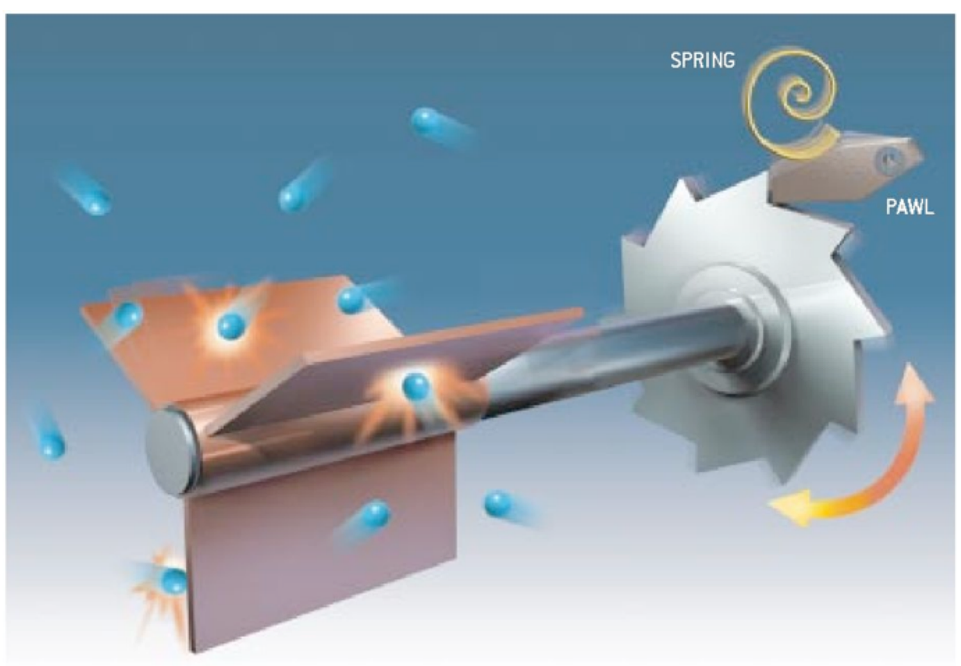

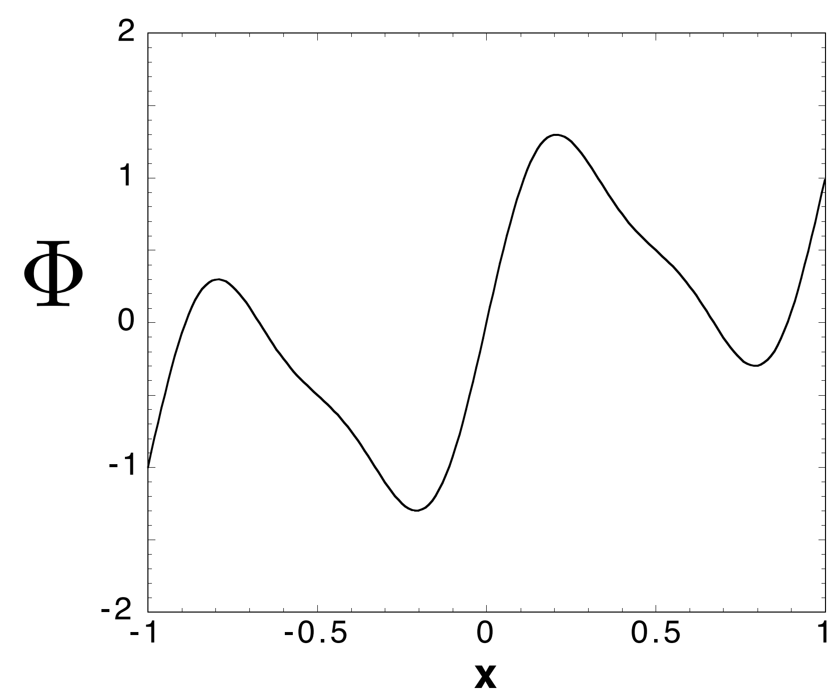

P. Reimann / Physics Reports 361 (2002) 57–265

1.6.1 Tilted Smoluchowski-Feynman ratchet

As a first example, assume that $F = const.$ and $D = const.$ This case can be considered as a (very) simple model for kinesin or dynein walking along a polar microtubule, with the constant force $F \geq 0$ accounting for the polarity. We would like to determine the mean transport velocity v_L for this model.

To evaluate Eq. (1.121), we focus on the long-time limit, noting that a stationary solution $p_\infty(x)$ of the corresponding FPE (1.118) must yield a constant current-density j_∞, i.e.,

$$j_\infty = -[(\partial_x \Phi) p_\infty + D \partial_x p_\infty] \tag{1.122}$$

where

$$\Phi(x) = U(x) - xF \tag{1.123}$$

is the full effective potential acting on the walker. By comparing with (1.85), one finds that the desired constant-current solution is given by

$$p_\infty(x) = \frac{1}{Z} e^{-\Phi(x)/D} \int_x^{x+L} dy \, e^{\Phi(y)/D}. \tag{1.124}$$

Constant current solution

$$v_L(t) := \frac{1}{N_L(t)} \int_0^L dx\, j(t,x) \;= \frac{1}{N_L(t)} \int_0^L dx\, [F(t) - U'(x)]\, p(t,x) \qquad j_\infty = -[(\partial_x \Phi) p_\infty + D \partial_x p_\infty]$$

$$p_\infty(x) = \frac{1}{Z}\, e^{-\Phi(x)/D} \int_x^{x+L} dy\, e^{\Phi(y)/D}. \tag{1.124}$$

This solution is spatially periodic, as can be seen from

$$\begin{aligned} p_\infty(x+L) &= \frac{1}{Z}\, e^{-[U(x+L)-(x+L)F]/D} \int_{x+L}^{x+2L} dy\, e^{[U(y)-yF]/D} \\ &= \frac{1}{Z}\, e^{-[U(x)-(x+L)F]/D} \int_x^{x+L} dz\, e^{[U(z+L)-(z+L)F]/D} \\ &= \frac{1}{Z}\, e^{-[U(x)-(x+L)F]/D} \int_x^{x+L} dz\, e^{[U(z)-(z+L)F]/D} \\ &= p_\infty(x), \end{aligned} \tag{1.125}$$

where we have used the coordinate transformation $z = y - L \in [x, x+L]$ after the first line.

$$v_L(t) := \frac{1}{N_L(t)} \int_0^L dx\, j(t,x) \;=\; \frac{1}{N_L(t)} \int_0^L dx\, [F(t) - U'(x)]\; p(t,x)$$

$$j_\infty = -[(\partial_x \Phi) p_\infty + D\partial_x p_\infty]$$

Inserting $p_\infty(x)$ into Eq. (1.121) gives

$$\begin{aligned} v_L &= -\frac{1}{N_L} \int_0^L dx\, (\partial_x \Phi)\, p_\infty \\ &= -\frac{1}{Z N_L} \int_0^L dx\, (\partial_x \Phi)\, e^{-\Phi(x)/D} \int_x^{x+L} dy\, e^{\Phi(y)/D} \\ &= \frac{D}{Z N_L} \int_0^L dx\, \left[\partial_x\, e^{-\Phi(x)/D}\right] \int_x^{x+L} dy\, e^{\Phi(y)/D}. \end{aligned} \tag{1.126}$$

$$v_L(t) := \frac{1}{N_L(t)}\int_0^L dx\, j(t,x) = \frac{1}{N_L(t)}\int_0^L dx\,[F(t)-U'(x)]\,p(t,x)$$

$$j_\infty = -[(\partial_x\Phi)p_\infty + D\partial_x p_\infty]$$

Inserting $p_\infty(x)$ into Eq. (1.121) gives

$$\begin{aligned} v_L &= -\frac{1}{N_L}\int_0^L dx\,(\partial_x\Phi)\,p_\infty \\ &= -\frac{1}{ZN_L}\int_0^L dx\,(\partial_x\Phi)\,e^{-\Phi(x)/D}\int_x^{x+L} dy\,e^{\Phi(y)/D} \\ &= \frac{D}{ZN_L}\int_0^L dx\,\left[\partial_x\,e^{-\Phi(x)/D}\right]\int_x^{x+L} dy\,e^{\Phi(y)/D}. \end{aligned} \tag{1.126}$$

Integrating by parts, this can be simplified to

$$\begin{aligned} v_L &= -\frac{D}{ZN_L}\int_0^L dx\,e^{-\Phi(x)/D}\partial_x\int_x^{x+L} dy\,e^{\Phi(y)/D} \\ &= -\frac{D}{ZN_L}\int_0^L dx\,e^{-\Phi(x)/D}\left[e^{\Phi(x+L)/D}-e^{\Phi(x)/D}\right] \\ &= \frac{D}{ZN_L}\int_0^L dx\,\left\{1-e^{[\Phi(x+L)-\Phi(x)]/D}\right\} \\ &= \frac{D}{ZN_L}\int_0^L dx\,\left\{1-e^{-F[(x+L)-x]/D}\right\} \\ &= \frac{DL}{ZN_L}\left(1-e^{-FL/D}\right), \end{aligned} \tag{1.127}$$

$$v_L(t) := \frac{1}{N_L(t)} \int_0^L dx\, j(t,x) \;=\; \frac{1}{N_L(t)} \int_0^L dx\, [F(t) - U'(x)]\; p(t,x)$$

$$j_\infty = -[(\partial_x \Phi) p_\infty + D \partial_x p_\infty]$$

$$v_L \;=\; \frac{DL}{Z N_L} \left(1 - e^{-FL/D}\right)$$

where N_L can be expressed as

$$N_L = \frac{1}{Z} \int_0^L dx \int_x^{x+L} dy\, e^{-[\Phi(x) - \Phi(y)]/D}. \tag{1.128}$$

We thus obtain the final result

$$v_L \;=\; DL\, \frac{1 - e^{-FL/D}}{\int_0^L dx\, \int_x^{x+L} dy\, e^{-[\Phi(x)-\Phi(y)]/D}}, \tag{1.129}$$

which holds for arbitrary periodic potentials $U(x)$. Note that there is no net-current at equilibrium $F = 0$.

Tilted Feynman-Smoluchowski ratchet

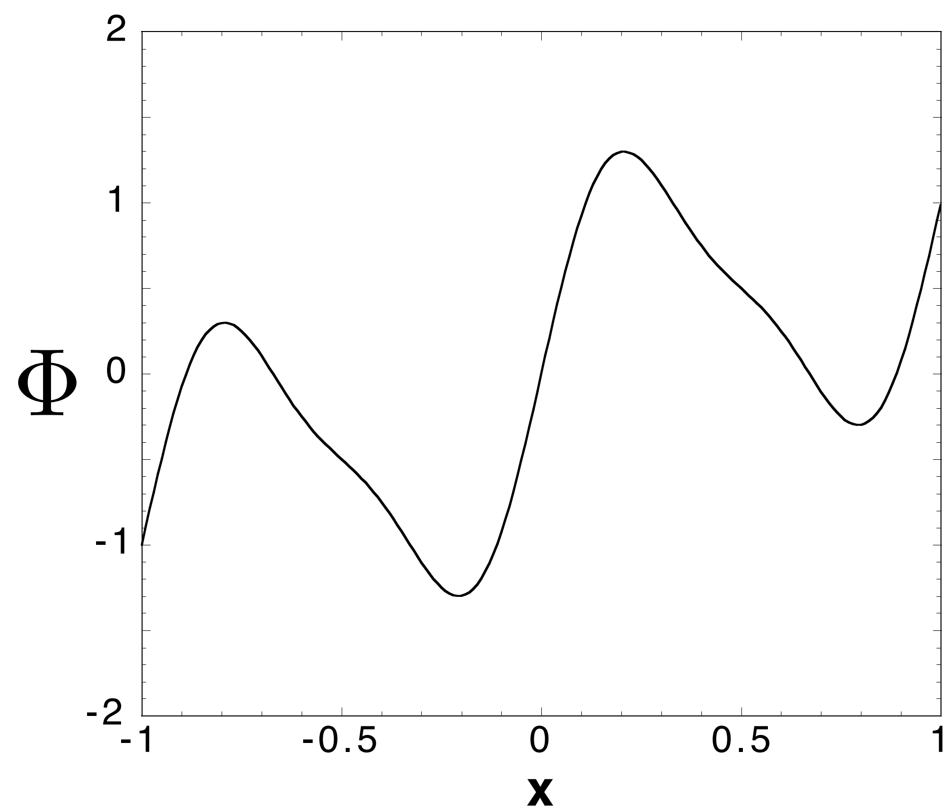

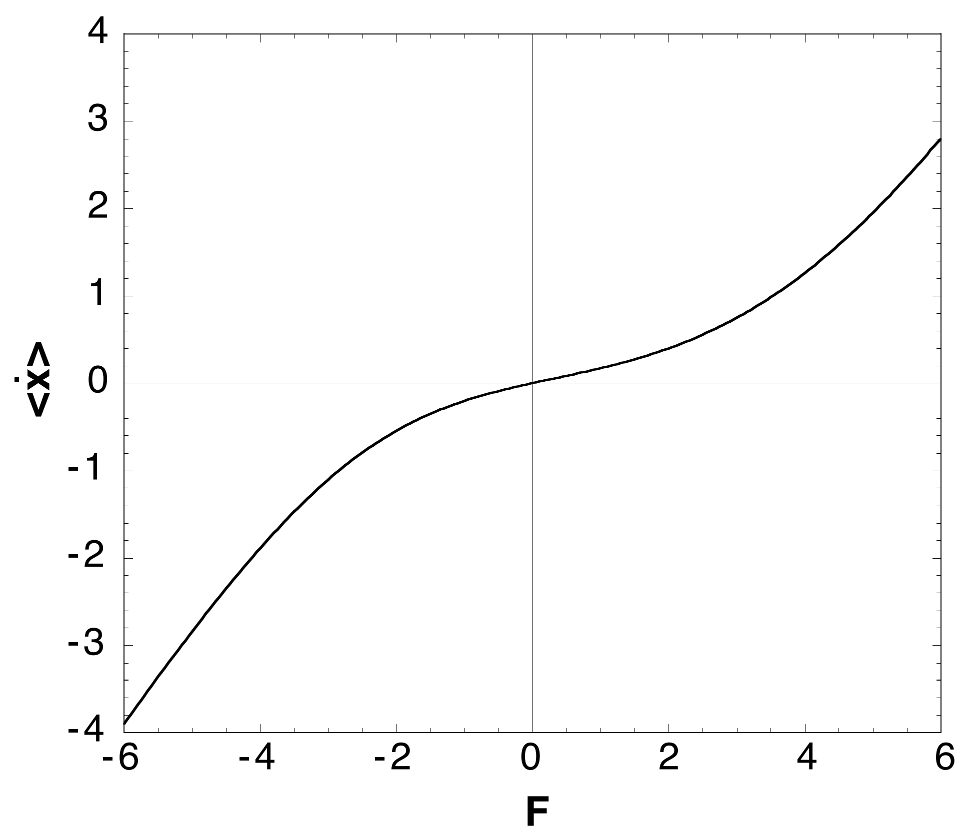

Fig. 2.3. Typical example of an effective potential from (2.35) "tilted to the left", i.e. $F<0$. Plotted is the example from (2.3) in dimensionless units (see Section A.4 in Appendix A) with $L=V_0=1$ and $F=-1$, i.e. $V_{\mathrm{eff}}(x)=\sin(2\pi x)+0.25\sin(4\pi x)+x$.

Fig. 2.4. Steady state current $\langle \dot{x} \rangle$ from (2.37) versus force F for the tilted Smoluchowski–Feynman ratchet dynamics (2.5), (2.34) with the potential (2.3) in dimensionless units (see Section A.4 in Appendix A) with $\eta = L = V_0 = k_{\mathrm{B}} = 1$ and $T=0.5$. Note the broken point-symmetry.

1.6.2 Temperature ratchet

As we have seen in the preceding sections, the combination of noise and nonlinear dynamics can yield surprising transport effects. Another example is the so-called temperature-ratchet, which can be captured by the minimal SDE model

$$dX(t) = [F - U'(X)]\, dt + \sqrt{2D(t)}\, dB(t), \tag{1.130a}$$

where $D(t) = D(t+T)$ is now a time-dependent noise amplitude, such as for instance

$$D(t) = \bar{D}\left\{1 + A\, \mathrm{sign}[\sin(2\pi t/T)]\right\}, \tag{1.130b}$$

where $|A| < 1$. Such a temporally varying noise strength can be realized by heating and cooling the ratchet system periodically. Transport can be quantified in terms of the combined spatio-temporal average

$$\begin{aligned} \langle \dot{X} \rangle &:= \frac{1}{T}\int_t^{t+T} ds \int_0^L dx\, j(t,x) \\ &= \frac{1}{T}\int_t^{t+T} ds \int_0^L dx\, [F - U'(x)]\, p(t,x). \end{aligned} \tag{1.131}$$

can be solved numerically

Time-dependent temperature

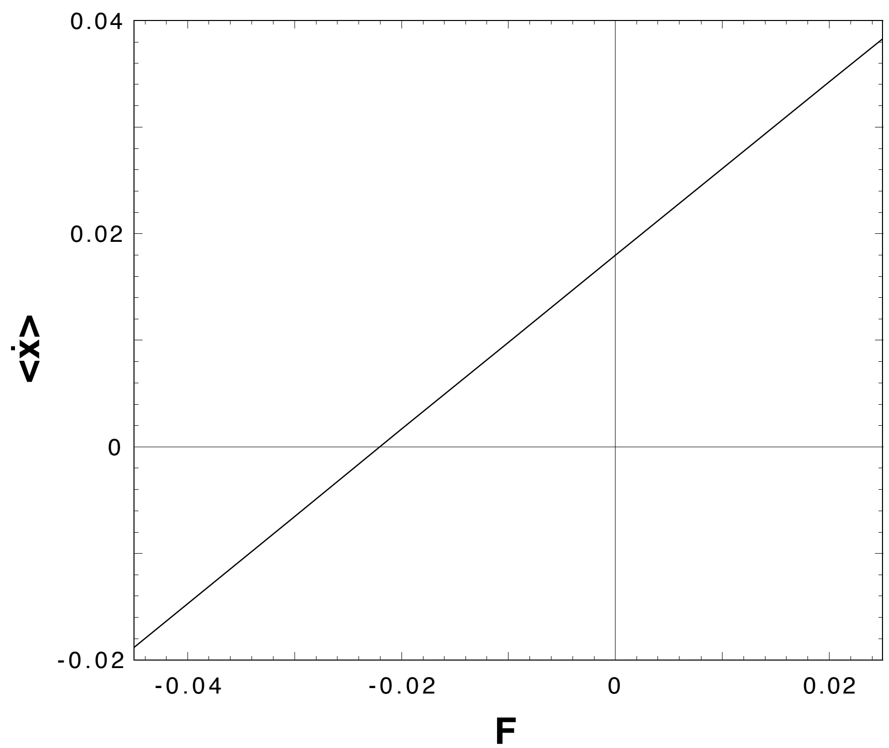

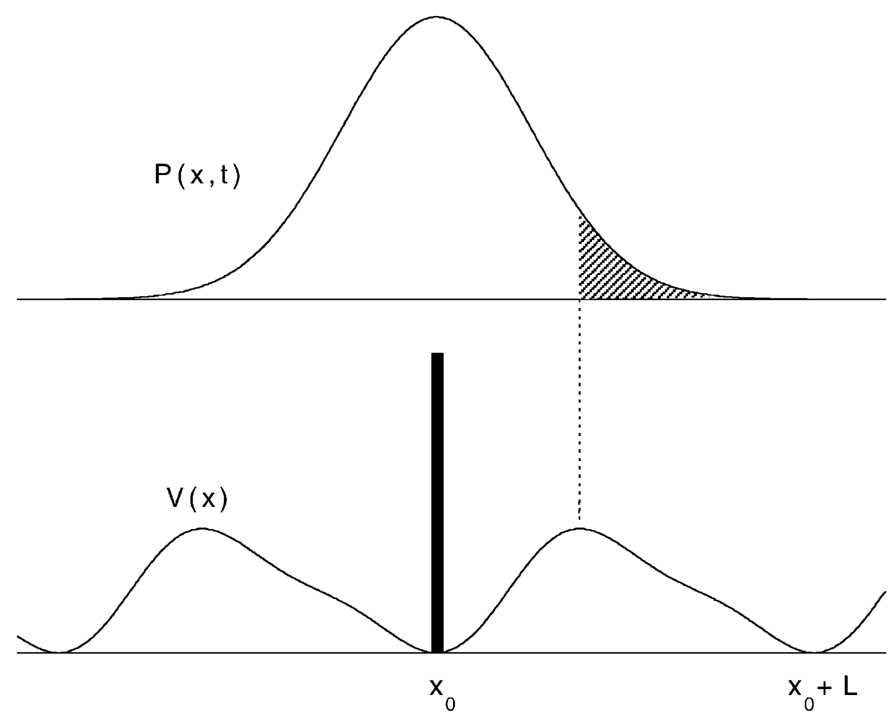

Fig. 2.5. Average particle current $\langle \dot{x} \rangle$ versus force F for the temperature ratchet dynamics (2.3), (2.34), (2.47), (2.50) in dimensionless units (see Section A.4 in Appendix A). Parameter values are $\eta = L = \mathscr{T} = k_B = 1$, $V_0 = 1/2\pi$, $\bar{T} = 0.5$, $A = 0.8$. The time- and ensemble-averaged current (2.53) has been obtained by numerically evolving the Fokker–Planck equation (2.52) until transients have died out.

Fig. 2.6. The basic working mechanism of the temperature ratchet (2.34), (2.47), (2.50). The figure illustrates how Brownian particles, initially concentrated at x_0 (lower panel), spread out when the temperature is switched to a very high value (upper panel). When the temperature jumps back to its initial low value, most particles get captured again in the basin of attraction of x_0, but also substantially in that of $x_0 + L$ (hatched area). A net current of particles to the right, i.e. $\langle \dot{x} \rangle > 0$ results. Note that practically the same mechanism is at work when the temperature is kept fixed and instead the potential is turned "on" and "off" (on–off ratchet, see Section 4.2).

dunkel@math.mit.edu